UNIVERSITÀ DEGLI STUDI DI URBINO CARLO BO

Department of: **BIOMOLECULAR SCIENCES**

Ph.D. PROGRAMME IN: **BIOMOLECULAR AND HEALTH SCIENCES**

CYCLE XXXVIII

NON-ALCOHOLIC FATTY LIVER DISEASE (NAFLD) AND UNDESERVED DECOMPRESSION SICKNESS (DCS) IN DIVERS: IS THERE A RELATIONSHIP?

ACADEMIC DISCIPLINES:

BIOS-12/A HUMAN ANATOMY
MEDS-02/B CLINICAL PATHOLOGY
MEDS-26/D ADVANCED MEDICAL AND SURGICAL TECHNOLOGY AND METHODOLOGY

Coordinator: Prof. Ferdinando Mannello

Supervisor: Prof. Pietro Gobbi

Co-Supervisor: Prof. Michela Battistelli

Ph.D. student: Dr. Andrea Galvani

ACADEMIC YEAR
2024/2025

INDEX

INTRODUCTION – RESEARCH HYPOTHESIS AND RATIONALE 9

CHAPTER 1 – EPIDEMIOLOGY AND PROFILES OF THE SUBJECTS INVOLVED: RECREATIONAL DIVING ACTIVITY AND NON-ALCOHOLIC FATTY LIVER DISEASE (NAFLD) 12

1. 1 General context and aims of the chapter 12
1. 2 Epidemiology and characteristics of recreational diving 12
1. 3 “Deserved” and “undeserved” decompression sickness: an epidemiological analysis 13
1. 4 Epidemiology of non-alcoholic fatty liver disease (NAFLD) 15
1. 5 Rationale for the convergence between recreational diving and NAFLD 17
..... **Errore. Il segnalibro non è definito.**
1. 6 Clinical and morphological framework of decompression sickness: deserved and undeserved forms 19
1. 7 Clinical classification: Type I and II DCS/DCI 19
1. 8 Classification by anatomical district involved 20
1. 9 Clinical - morphological correlation between “deserved” and “undeserved” DCS 21
1. 10 Interpretative synthesis and pathophysiological perspective 22

CHAPTER 2 – MORPHOLOGY AND HISTOLOGY OF HEPATIC TISSUE AND VASCULAR ENDOTHELIUM UNDER PHYSIOLOGICAL CONDITIONS 23

2. 1 Anatomical and physiological context of the chapter 23
2. 2 Structure and function of the vascular endothelium under physiological conditions 23
2. 3 Anatomy and histology of healthy hepatic tissue 26

CHAPTER 3 – MORPHOLOGICAL AND HISTOLOGICAL ALTERATIONS OF THE HEPATOCYTE AND HEPATIC TISSUE IN NON-ALCOHOLIC FATTY LIVER DISEASE (NAFLD) 28

3. 1 General framework and objectives of the chapter 28
3. 2 Morphological and histological aspects of the steatotic hepatocyte 28
3. 3 Histological classification and grading of hepatic steatosis 30

CHAPTER 4 - ULTRASOUND DIAGNOSTIC ASPECTS OF NAFLD 32

4. 1 Complementary techniques and diagnostic innovations in the ultrasound assessment of NAFLD 32
4. 2 Hepato-renal index (HRI) and quantification of steatosis 32
4. 3 Controlled attenuation parameter (CAP) and elastographic integration 33
4.3.1 Quantitative ultrasound and advanced steatometry 33
4.3.2 Methodological considerations and future perspectives 34

CHAPTER 5 – PATHOPHYSIOLOGICAL AND MORPHOLOGICAL ASPECTS OF BUBBLE FORMATION DURING SCUBA DIVING 35

5. 1 General framework of decompression pathophysiology 35
5. 2 Micronuclei and “Active Hydrophobic Spots” (AHS) 36
5. 3 Systemic pathophysiology of the bubble 37
5. 4 Individual variability in bubble production 38
5. 5 Key points for the research project 39

CHAPTER 6 – EXPERIMENTAL SECTION 40

6. 1 In vitro experimental models and pathophysiological rationale 40

6.1.1 In vitro models for the reproduction of hepatic steatosis: cell lines, approaches, and experimental rationale 41
6.1.2 IL-6 production in the cellular model of induced hepatic steatosis....42
6.1.3 Inflammatory patterns and molecular mediators in steatotic cells: potential links with DCS 44
6. 2 In vivo experimental study in recreational divers: design and methodology....46
6.2.1 Dry hyperbaric chamber dive design and sample selection 46
6.2.2 Pre-dive clinical and hepatic ultrasound assessment....47
6.2.3 Simulated “dry” dive in hyperbaric chamber 48
6.2.4 Post-dive cardiac and vascular ultrasound assessment for bubble detection 49
6. 3 Ultrasound detection of venous gas emboli (VGE): pathophysiological rationale and methodological validity 50
6. 4 Scientific foundations and methodological rationale for ultrasound use 51
6. 5 Individual variability in bubble production....51
6. 6 Correlation between bubble density and DCS risk 51
6. 7 Safety, reproducibility, and applicability in operational settings 52
6. 8 Purpose of post-dive cardiac and vascular ultrasound 52
6. 9 Pathophysiological rationale: NAFLD, chronic inflammation, and endothelial vulnerability 53
CHAPTER 7 – STATISTICAL ANALYSIS....54
7. 1 Materials and methods – Study design and participants 54
7.1.1 Variables 54
7.1.2 Statistical analysis 55
7. 2 Results 56
7.2.1 Descriptive statistics....56
7.2.2 Descriptive comparison of bubble count in relation to NAFLD presence 56
....57
....57
7.2.3 Correlations and multicollinearity....57
7.2.4 ANCOVA model selection....57
7.2.5 Model quality 58
7.2.6 Analysis of variance 58
7.2.7 Model parameters 58
7.2.8 Estimated marginal means....59
7. 3 Interpretation of the results 60
7. 4 Figures and graphs 61
CHAPTER 8 – DISCUSSION OF THE RESULTS....75
8. 1 Pathophysiological framework and biological rationale....75
8. 2 Results of the in vivo study: individual variability and associated factors 75
8. 3 Integration with the multivariate statistical model....76
8. 4 Contribution of the in vitro study and biological coherence....77
8. 5 Role of IL-6 as a possible pathophysiological link between NAFLD and decompression sickness 77
CHAPTER 9 – CONCLUSION....79

LIST OF FIGURES

Figure 1 – Scuba Diver in Blue Diver underwater. Source: Photowall, Scuba Diver in Blue ..10

Figure 2 – Spectrum of non-alcoholic fatty liver disease (NAFLD) progression. Source: Webflow CDN, 2023 11

Figure 1.1 – Estimated prevalence of NAFLD in the adult population by geographical area. Source: our own elaboration based on global epidemiological data.....15

Figure 1.2 – Ultrasound appearance of non-alcoholic fatty liver disease (NAFLD): diffuse increase in parenchymal echogenicity with posterior attenuation of the ultrasound beam. Source: POCUS.org, Liver Ultrasound – Fatty Liver Disease, 2025.....18

Figure 1.3 – Pathophysiological scheme of decompression sickness. Source: own elaboration (2025).....22

Figure 2.1 – Vascular endothelium: a single layer of elongated squamous cells lining the inner surface of blood vessels. Source: M. Megías, Histology and Cell Biology – University of Vigo (CC BY-NC-SA 4.0 license).....24

Figure 2.2 – Hepatic sinusoidal endothelium (Liver Sinusoidal Endothelial Cells, LSEC) observed by scanning electron microscopy: the characteristic fenestrations enabling selective exchange between blood and the space of Disse are visible. Source: adapted from Poisson J. et al., Liver Sinusoidal Endothelial Cells: Physiology and Role in Liver Diseases, Frontiers in Physiology, 2021 (12:735573), doi:10.3389/fphys.2021.735573.....25

Figure 2.3 – Schematic representation of the hepatic sinusoid: the fenestrated sinusoidal endothelium allows the passage of molecules between the blood and hepatocytes through the space of Disse; Kupffer cells and hepatic stellate cells (Ito cells) are also visible. Source: adapted from Sørensen K.K. et al., The Scavenger Cells of the Liver – The Liver Sinusoidal Endothelial Cell and the Kupffer Cell, Frontiers in Physiology, 2019 (10:1032), doi:10.3389/fphys.2019.01032. CC BY 4.0 license.....27

Figure 3.1 – Comparison between microvesicular (A) and macrovesicular (B) hepatic steatosis. In the microvesicular form, hepatocytes show numerous small lipid vacuoles, with a central nucleus and finely granular cytoplasm; in the macrovesicular form, the single large lipid droplet displaces the nucleus to the periphery of the cell. Source: adapted from Younossi Z.M. et al., Histopathology of Non-alcoholic Fatty Liver Disease and Steatohepatitis, World Journal of Gastroenterology, 2014; 20(42):15019–15029.....29

Figure 5.1 – Illustrative diagram of the pathogenesis of decompression sickness (Decompression Sickness). Source: adapted from Lecturio Medical Education – Decompression Sickness (DCS), 2023.....36

Figure 5.2 – Interaction between intravascular gas bubbles and the vascular endothelium. Source: adapted from Thom S. R. et al., Frontiers in Immunology, 2023, 14:1230049. DOI: 10.3389/fimmu.2023.1230049.....38

Figure 6.1 – Production of the pro-inflammatory cytokine IL-6 in control HepG2 cells and in cells with induced NAFLD. Source: original graph drawn based on assessments conducted on cell samples cultured at the laboratories of the University of Urbino Carlo Bo – Enrico Mattei Campus (2022–2025).....43

Figure 6.2 – A–B: Control HepG2 cells. C–D: HepG2 cells treated with palmitic acid and oleic acid. In treated samples C and D, the intracellular accumulation of clear lipid-containing vesicles is evident; these occupy part of the cellular volume and leave impressions on larger organelles, such as the nucleus in C. Arrow = mitochondrial degeneration. Source: original images acquired in the laboratory at the University of Urbino Carlo Bo – Enrico Mattei Campus (2023) 45

Figure 6.3 – Graph showing the dry hyperbaric chamber dive profile used during the research project tests to simulate a standardized underwater dive at 30 meters. Source: 'Domus Medica' Hyperbaric Medicine Center – Republic of San Marino (2024).....49

Figure 7.1– Comparison of the number of ultrasound-detected bubbles in relation to the presence of NAFLD. The graph shows the distribution of the number of bubbles detected at echocardiographic examination (y-axis) in subjects without NAFLD (absence, left) and with NAFLD (presence, right), allowing a comparison between the two groups. Source: statistical data processing by Prof. Davide Sisti, Department of Biomolecular Sciences (DISB), University of Urbino Carlo Bo (2025).....57

Figure 7.2 – Box plot of the distribution of NAFLD eco2 values detected using a fixed ultrasound system. The box plot represents the distribution of NAFLD eco2 values, highlighting the minimum value, the first and third quartiles, the median, and the possible presence of outliers. Source: statistical data processing by Prof. Davide Sisti, Department of Biomolecular Sciences (DISB), University of Urbino Carlo Bo (2025).....62

Figure 7.3 – Box plot of the distribution of ecoCARDIO (bubble) values. The box plot represents the distribution of ecoCARDIO values, highlighting the minimum value, the first and third quartiles, the median, and the range of observed values, allowing an assessment of the variability of the measurement in the analyzed sample. Source: statistical data processing by Prof. Davide Sisti, Department of Biomolecular Sciences (DISB), University of Urbino Carlo Bo (2025) 62

Figure 7.4 – Box plot of the age distribution of the study sample. The box plot represents the distribution of age values, highlighting the minimum value, the first and third quartiles, the median, and the range of observed values, allowing an assessment of the demographic variability of the analyzed sample. Source: statistical data processing by Prof. Davide Sisti, Department of Biomolecular Sciences (DISB), University of Urbino Carlo Bo (2025) 63

Figure 7.5 – Box plot of the distribution of body weight (kg) of the study sample. The box plot represents the distribution of body weight values, highlighting the minimum value, the first and third quartiles, the median, and the range of observed values, allowing an assessment of the weight variability of the analyzed sample. Source: statistical data processing by Prof. Davide Sisti, Department of Biomolecular Sciences (DISB), University of Urbino Carlo Bo (2025) 63

Figure 7.6– Box plot of the distribution of body mass index (BMI) of the study sample. The box plot represents the distribution of BMI values, highlighting the minimum value, the first and third quartiles, the median, and the range of observed values, allowing an assessment of the variability of weight status in the analyzed sample. Source: statistical data processing by Prof. Davide Sisti, Department of Biomolecular Sciences (DISB), University of Urbino Carlo Bo (2025) 64

Figure 7.7 – Box plot of the distribution of height (cm) of the study sample. The box plot represents the distribution of height values, highlighting the minimum value, the first and third quartiles, the median, and the range of observed values, allowing an assessment of the stature variability of the analyzed sample. Source: statistical data processing by Prof. Davide Sisti, Department of Biomolecular Sciences (DISB), University of Urbino Carlo Bo (2025) 64

Figure 7.8 – Relative frequency of subjects with an average annual number of dives between 0 and 10. Category 0 indicates the absence of dives in this range, while category 1 indicates the presence

of dives in this range. Source: statistical data processing by Prof. Davide Sisti, Department of Biomolecular Sciences (DISB), University of Urbino Carlo Bo (2025) 66

Figure 7.9 – Relative frequency of subjects with an average annual number of dives between 10 and 20. Category 0 indicates subjects who do not belong to this range, while category 1 indicates subjects who belong to this range. Source: statistical data processing by Prof. Davide Sisti, Department of Biomolecular Sciences (DISB), University of Urbino Carlo Bo (2025) 66

Figure 7.10 – Relative frequency of subjects with an average annual number of dives greater than 20. Category 0 indicates subjects who do not belong to this range, while category 1 indicates subjects who belong to this range. Source: statistical data processing by Prof. Davide Sisti, Department of Biomolecular Sciences (DISB), University of Urbino Carlo Bo (2025) 67

Figure 7.11 – Relative frequency of subjects in relation to smoking habit. Category 0 indicates non-smokers, while category 1 indicates smokers. Source: statistical data processing by Prof. Davide Sisti, Department of Biomolecular Sciences (DISB), University of Urbino Carlo Bo (2025) 67

Figure 7.12 – Relative frequency of subjects in relation to the presence of arterial hypertension. Category 0 indicates subjects who do not report arterial hypertension, while category 1 indicates subjects who report having it. Source: statistical data processing by Prof. Davide Sisti, Department of Biomolecular Sciences (DISB), University of Urbino Carlo Bo (2025) 68

Figure 7.13 – Relative frequency of subjects in relation to the presence of cardiovascular diseases. Category 0 indicates subjects who do not report the presence of cardiovascular diseases, while category 1 indicates subjects who report their presence. Source: statistical data processing by Prof. Davide Sisti, Department of Biomolecular Sciences (DISB), University of Urbino Carlo Bo (2025) 68

Figure 7.14 – Relative frequency of subjects in relation to the presence of metabolic diseases. Category 0 indicates subjects who do not report the presence of metabolic diseases, while category 1 indicates subjects who report their presence. Source: statistical data processing by Prof. Davide Sisti, Department of Biomolecular Sciences (DISB), University of Urbino Carlo Bo (2025) 69

Figure 7.15 – Relative frequency of subjects in relation to the presence of first-degree family history of the considered diseases. Category 0 indicates subjects who do not report a first-degree family history of the considered diseases, while category 1 indicates subjects who report the presence of at least one affected first-degree relative. Source: statistical data processing by Prof. Davide Sisti, Department of Biomolecular Sciences (DISB), University of Urbino Carlo Bo (2025) 69

Figure 7.16 – Relative frequency of subjects in relation to blood glucose levels. Category 0 indicates subjects who do not report altered glycemic values, while category 1 indicates subjects who report altered glycemic values. Source: statistical data processing by Prof. Davide Sisti, Department of Biomolecular Sciences (DISB), University of Urbino Carlo Bo (2025) 70

Figure 7.17– Relative frequency of subjects in relation to lipid profile. Category 0 indicates subjects who do not report alterations in lipid profile, while category 1 indicates subjects who report alterations in lipid profile. Source: statistical data processing by Prof. Davide Sisti, Department of Biomolecular Sciences (DISB), University of Urbino Carlo Bo (2025) 70

Figure 7.18 – Relative frequency of subjects in relation to liver profile. Category 0 indicates subjects who do not report alterations in liver profile, while category 1 indicates subjects who report alterations in liver profile. Source: statistical data processing by Prof. Davide Sisti, Department of Biomolecular Sciences (DISB), University of Urbino Carlo Bo (2025) 71

Figure 7.19 – Relative frequency of subjects in relation to the use of medications for cardiovascular diseases. Category 0 indicates subjects who do not take medications for cardiovascular diseases, while category 1 indicates subjects who take medications for cardiovascular diseases. Source: statistical data processing by Prof. Davide Sisti, Department of Biomolecular Sciences (DISB), University of Urbino Carlo Bo (2025).....71

Figure 7.20 – Relative frequency of subjects in relation to the use of medications for diabetes. Category 0 indicates subjects who do not take medications for diabetes, while category 1 indicates subjects who take medications for diabetes. Source: statistical data processing by Prof. Davide Sisti, Department of Biomolecular Sciences (DISB), University of Urbino Carlo Bo (2025) 72

Figure 7.21 – Relative frequency of subjects in relation to the use of medications for dyslipidemia. Category 0 indicates subjects who do not take medications for dyslipidemia, while category 1 indicates subjects who take medications for dyslipidemia. Source: statistical data processing by Prof. Davide Sisti, Department of Biomolecular Sciences (DISB), University of Urbino Carlo Bo (2025).....72

Figure 7.22 – Relative frequency of subjects in relation to the use of medications for joint diseases. Category 0 indicates subjects who do not take medications for joint diseases, while category 1 indicates subjects who take medications for joint diseases. Source: statistical data processing by Prof. Davide Sisti, Department of Biomolecular Sciences (DISB), University of Urbino 'Carlo Bo' (2025).....73

Figure 7.23 – Relative frequency of subjects in relation to the use of medications for gastrointestinal diseases. Category 0 indicates subjects who do not take medications for gastrointestinal diseases, while category 1 indicates subjects who take medications for gastrointestinal diseases. Source: statistical data processing by Prof. Davide Sisti, Department of Biomolecular Sciences (DISB), University of Urbino 'Carlo Bo' (2025).....73

Figure 7.24 – Relative frequency of subjects in relation to the use of medications for urological diseases. Category 0 indicates subjects who do not take medications for urological diseases, while category 1 indicates subjects who take medications for urological diseases. Source: statistical data processing by Prof. Davide Sisti, Department of Biomolecular Sciences (DISB), University of Urbino Carlo Bo (2025).....74

LIST OF TABLES

Table 1.1- Epidemiological indicators and global diffusion of recreational diving. Source: own elaboration based on PADI data and sector literature 16

Table 1.2 – Prevalence, geographical distribution, and estimated incidence of NAFLD in the adult population. Source: Ballestri et al. (2017) and indexed literature (PMC) 17

Table 3.1- Histological grading of hepatic steatosis based on the extent of hepatocyte involvement. Source: adapted from Brunt et al., *Nonalcoholic fatty liver disease: histopathologic features and clinical correlations*, Hepatology, 1999, and subsequent revisions. 31

Table 7.1 – Results of the analysis of covariance (ANCOVA) on the number of echocardiographic microbubbles. Source: statistical data processing by Prof. Davide Sisti, Department of Biomolecular Sciences (DISB), University of Urbino Carlo Bo (2025). 58

Table 7.2 – Coefficients of the regression model (ANCOVA) for the number of echocardiographically detected microbubbles (ecoCARDIO). Source: statistical data processing by Prof. Davide Sisti, Department of Biomolecular Sciences (DISB), University of Urbino Carlo Bo (2025) 59

Table 7.3 – Descriptive statistics of the analyzed quantitative variables. Source: statistical data processing by Prof. Davide Sisti, Department of Biomolecular Sciences (DISB), University of Urbino Carlo Bo (2025) 61

Table 7.4 – Descriptive statistics of the qualitative variables of the sample. Source: statistical data processing by Prof. Davide Sisti, Department of Biomolecular Sciences (DISB), University of Urbino Carlo Bo (2025). 65

Introduction – Research hypothesis and rationale

Decompression sickness (DCS) is a rare but potentially severe clinical condition caused by the formation of inert gas bubbles in tissues and in the bloodstream, primarily nitrogen, during ascent to the surface[1].

Despite the widespread adoption of standardized decompression tables and well-established conservative ascent algorithms, approximately 60% of documented DCS cases occur in individuals who strictly adhere to decompression protocols; these events are known as "undeserved" DCS, the etiopathogenesis of which remains only partially elucidated[2].

In recent years, scientific attention has increasingly shifted toward the influence of individual physiological and metabolic factors that may predispose to undeserved DCS, with particular interest in all subclinical conditions capable of altering the vascular and inflammatory response of the human body to environments with increased ambient pressure, such as (but not limited to) scuba diving. Among these, considerable attention has been devoted to cardiovascular and metabolic diseases and patterns; for example, the endothelium is unquestionably one of the tissues most "challenged" during underwater exposure. A possible association has been hypothesized with non-alcoholic fatty liver disease (NAFLD), one of the most prevalent chronic liver diseases in the Western world, with an estimated prevalence of up to 30% in the general population[3].

NAFLD is no longer regarded as an isolated hepatic disorder, but rather as a systemic manifestation of metabolic syndrome, strongly associated with chronic low-grade inflammation, insulin resistance, endothelial dysfunction, hypercoagulability, and increased cardiovascular risk[4]-[5]. These pathogenetic processes show striking similarities to the pathophysiological mechanisms induced by gas bubbles in

[1] Vann R. D., Butler F. K., Mitchell S. J., Moon R. E. (2011). *Decompression Illness. Lancet*, 377(9760), 153–164.
[2] Gempp E., Blatteau J. E. (2010). *Prevalence of Decompression Sickness in Recreational Diving: A Review of Contributing Factors. Undersea & Hyperbaric Medicine*, 37(3), 133–140.
[3] Dinani A., Sanyal A. J. (2017). *Nonalcoholic Fatty Liver Disease: Epidemiology, Pathogenesis, and Treatment. Clinics in Liver Disease*, 21(2), 301–312.
[4] Liu W., Baker R. D., Bhatia T., Zhu L., Baker S. S. (2010). *Pathogenesis of Nonalcoholic Steatohepatitis. Cellular and Molecular Life Sciences*, 67(19), 3327–3342.
[5] Xu R., Tao A., Zhang S., Chen G. (2024). *NAFLD and Endothelial Dysfunction: Mechanisms Linking Liver and Vascular Disease. Frontiers in Cardiovascular Medicine*, 11, 1378945.

DCS, which in turn lead to endothelial injury, activation of inflammatory cascades, and intravascular coagulation—the same elements that characterize the early stages of NAFLD[6].

Figure 1 – *Scuba Diver in Blue Diver underwater.*
Source: Photowall, Scuba Diver in Blue

Recent studies further suggest that an enhanced systemic inflammatory response or alterations in microcirculatory function may promote bubble formation or slow their clearance, thereby increasing individual susceptibility to DCS even during properly conducted dives[7]. From this perspective, NAFLD may therefore represent a latent and underrecognized risk factor for the development of "undeserved" forms of DCS, particularly among adult recreational divers.

[6] Azizov A., Schwarz N., Bäuerle T., et al. (2013). *Endothelial Injury and Inflammation in Decompression Illness: Parallels with Metabolic Liver Disease. PLoS One*, 8(12), e83235.
[7] Cialoni D., Pieri M., Marroni A., et al. (2017). *Physiological Predisposition to Decompression Sickness: The Role of Endothelial Function and Microcirculation. Frontiers in Physiology*, 8, 1063.

Beyond its biological relevance, the high prevalence and often asymptomatic nature of NAFLD, together with the ease of diagnosis through liver ultrasonography, make this condition an ideal candidate for targeted screening programs in divers. The early identification of individuals with hepatic steatosis—should such a relationship be confirmed—could open the way to personalized preventive strategies, ultimately improving diving safety and decompression risk management.

Within this framework, the present doctoral thesis aims to investigate, through both in vitro and in vivo experimental models, the existence of a biologically and clinically significant correlation between NAFLD and "undeserved" DCS, with the objective of contributing to the identification of novel biomarkers of individual susceptibility and promoting the evolution of diving medicine toward an increasingly predictive and personalized approach.

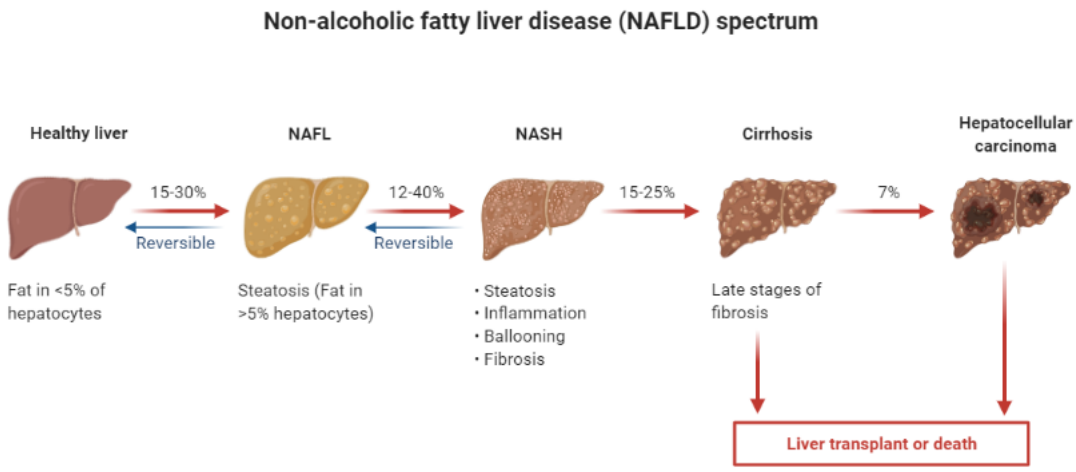

Figure 2 – *Spectrum of non-alcoholic fatty liver disease (NAFLD) progression.* Source: Webflow CDN, 2023

Chapter 1 – Epidemiology and profiles of the subjects involved: recreational diving activity and non-alcoholic fatty liver disease (NAFLD)

1. 1 General context and aims of the chapter

This chapter outlines the epidemiological and clinical background of two key domains of the research project: recreational scuba diving activity and non-alcoholic fatty liver disease (NAFLD). The objective is twofold: on the one hand, to describe the diffusion and demographic characteristics of the recreational diving population; on the other, to illustrate the epidemiological and clinical relevance of NAFLD as a metabolic condition of increasing impact. These two domains, only apparently distinct, constitute the framework within which the research hypothesis is embedded: the easily diagnosable presence of NAFLD (by means of simple abdominal ultrasound) could represent a factor of pathophysiological vulnerability with respect to the potentially increased risk of developing "undeserved" decompression sickness (DCS), that is, forms that occur despite compliance with safety protocols, particularly decompression stops and ascent rate limits[8].

1. 2 Epidemiology and characteristics of recreational diving

Over the past decades, recreational scuba diving has experienced steady global growth, both in terms of the number of practitioners and the expansion of operational infrastructures. The Professional Association of Diving Instructors (PADI) reports that, since 1967, more than 28 million certifications have been issued in 186 countries, underscoring the widespread nature of the phenomenon[9].

In the United States, approximately 3.1 million individuals declared that they had engaged in diving at least once during 2014, corresponding to 1.1% of the adult population[10]. At the global level, in the most recent five-year period an average annual growth rate of 1.8% in newly certified divers has been estimated. Two main categories of divers can be identified:

---

[8] Vann R. D., Butler F. K., Mitchell S. J., Moon R. E. (2011). *Decompression Illness. Lancet*, 377(9760), 153–164.
[9] Professional Association of Diving Instructors (PADI). *Annual Certification and Industry Statistics Report.* 2023.
[10] Divers Alert Network (DAN). *Annual Diving Report 2014–2015.* Durham, NC: DAN Publications, 2016.

- **Casual divers**, occasional practitioners, showing an annual increase of 2.7%;
- **Core divers**, regular and more experienced divers, who instead display a slight decline.

Despite the potentially hazardous nature of the activity, the mortality rate associated with recreational diving remains relatively low: in the United States, approximately 2 deaths per 1,000,000 dives per year are estimated[11].

Nevertheless, the occurrence of decompression sickness (DCS) in individuals who have strictly adhered to decompression tables and ascent procedures - a phenomenon defined as "undeserved" - raises particular clinical interest[12]. This observation suggests the possible presence of individual risk factors that are not yet fully elucidated, of a physiological, metabolic, or endothelial nature, which could modulate the organism's response to changes in ambient pressure.

1. 3 "Deserved" and "undeserved" decompression sickness: an epidemiological analysis

Decompression sickness (DCS, or Patologie da decompressione) represents a complex pathophysiological phenomenon, described since the earliest hyperbaric experiments of the nineteenth century and still the subject of intense clinical and experimental investigation. From an epidemiological perspective, the analysis of data collected by the Divers Alert Network (DAN) and other international agencies specialized in the monitoring of diving incidents makes it possible to delineate a precise quantitative framework of the incidence and distribution of DCS in both recreational and technical diving contexts.

According to the most recent data[13], the average incidence of DCS events among recreational divers is approximately 1 case every 5,000–10,000 dives, with higher rates observed among technical and professional divers. Analyses conducted on the Diving Safety Laboratory (DSL) database of DAN Europe, which includes thousands of controlled dives, have enabled the identification of two main categories of events: **"deserved" decompression sickness**, in which violations of decompression

[11] Buzzacott P., Denoble P. J., et al. (2018). *Diving Fatalities in Recreational Scuba Diving: Epidemiology and Risk Factors.Undersea & Hyperbaric Medicine*, 45(4), 383–392.
[12] Gempp E., Blatteau J. E. (2010). *Prevalence of Decompression Sickness in Recreational Diving: A Review of Contributing Factors. Undersea & Hyperbaric Medicine*, 37(3), 133–140.
[13] DAN Annual Diving Report 2023. Divers Alert Network Europe. https://www.daneurope.org

protocols are documented (excessively rapid ascents, omitted stops, incorrect use of breathing gases, or repeated dives with inadequate surface intervals), and **"undeserved" forms**, which occur despite strict adherence to the prescribed decompression tables and profiles[14].

This distinction, while apparently straightforward, has important interpretative implications. "Deserved" cases are currently decreasing due to the widespread use of dive computers, adaptive decompression algorithms, and advanced diver training, whereas "undeserved" forms have gained increasing prominence, accounting, according to some estimates, for 20% to 30% of total cases[15]; according to others, even **higher figures of up to 60%** have been reported.

This phenomenon suggests that, beyond operational variables, individual predisposing factors - including endothelial dysfunction, chronic low-grade systemic inflammation, genetic polymorphisms, alterations in lipid metabolism, and chronic conditions such as non-alcoholic fatty liver disease (NAFLD) - may modulate the organism's response to hyperbaric stress and the subsequent formation of gas bubbles in body tissues.

Epidemiological evidence, supported by multicenter prospective studies, also demonstrates marked interindividual variability in the production of **venous gas emboli (VGE)** under standardized diving conditions. Some individuals, defined as "bubble-prone," generate large amounts of bubbles while remaining asymptomatic, confirming the crucial role of endothelial and microcirculatory physiology in determining decompression risk.

Overall, the distinction between deserved and undeserved DCS does not represent merely a descriptive classification, but constitutes an essential step toward a predictive and personalized model of diving medicine, in which the diver's biological and metabolic profile becomes a determinant of risk at least as important as the technical parameters of the dive.

---

[14] Cialoni D., Pieri M., Balestra C., Marroni A. *Dive Risk Factors, Gas Bubble Formation, and Decompression Illness in Recreational SCUBA Diving: Analysis of DAN Europe DSL Database. Front Psychol.* 2017;8:1587.

[15] Imbert J.P., Egi S.M., Germonpré P., Balestra C. *Static Metabolic Bubbles as Precursors of Vascular Gas Emboli During Divers' Decompression. Front Physiol.* 2019; 10:807

1. 4 Epidemiology of non-alcoholic fatty liver disease (NAFLD)

NAFLD currently represents the most common form of chronic liver disease in industrialized countries and, increasingly, also in developing ones. Global estimates indicate an average **prevalence of 25% in the adult population**, with significant geographic variations: approximately 14% in Africa, 23% in Europe, 24% in the United States, 27% in Asia, 31% in South America, and 32% in the Middle East[16].

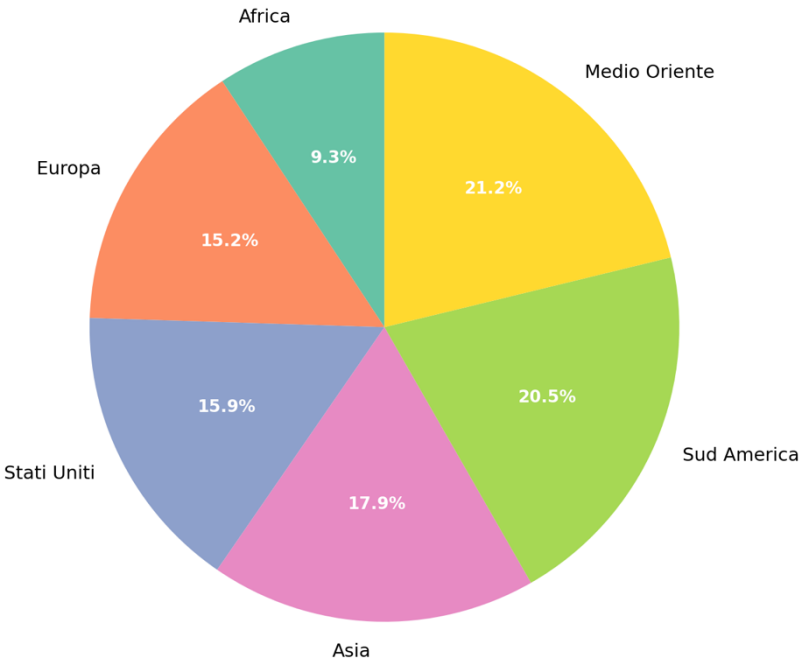

Figure 1.1 – *Estimated prevalence of NAFLD in the adult population by geographical area.* Source: our own elaboration based on global epidemiological data

From a pathophysiological standpoint, NAFLD is no longer considered a mere condition of intrahepatic lipid accumulation, but rather a systemic disease associated with metabolic dysfunction, insulin resistance, obesity, dyslipidemia, arterial hypertension, and increased cardiovascular risk[17].

[16] Younossi Z. M., et al. (2019). *Global Epidemiology of Nonalcoholic Fatty Liver Disease. Nature Reviews Gastroenterology & Hepatology*, 16(1), 11–20.
[17] Marchesini G., Day C. P., et al. (2016). *Pathogenesis of NAFLD: Metabolic, Genetic, and Environmental Factors.Journal of Hepatology*, 64(2), 696–708.

Recent meta-analyses have confirmed that NAFLD is associated with an increased risk of cardiovascular events, even in the absence of advanced liver fibrosis[18].

In a prospective cohort study, **the incidence of cardiovascular events was 2.82 per 1,000 person-years in subjects with NAFLD, compared with 0.97 in healthy controls**[19].

Furthermore, the condition has been identified as an independent risk factor for cardiovascular diseases even in non-obese individuals, suggesting that hepato-metabolic dysfunction may autonomously contribute to endothelial and microvascular impairment[20].

From a clinical perspective, the diagnosis of NAFLD is relatively straightforward, relying simply on liver ultrasound, biochemical analyses, and metabolic profiles. However, the condition is often asymptomatic, resulting in a substantial proportion of **underdiagnosis** in the general population[21].

Table 1.1- *Epidemiological indicators and global diffusion of recreational diving.* Source: own elaboration based on PADI data and sector literature

Indicator	Value / description	Comments
Total number of certifications issued by the Professional Association of Diving Instructors (PADI) since 1967	> 28 million + (PADI)	Refers to the PADI organization as a proxy for the global diffusion of recreational diving
Operating countries/territories	186 countries/territories (PADI Blog)	"Certifications issued in 186 countries"
Estimated percentage of the U.S. population that had dived at least once in 2014	Approximately 1.1%	U.S. data, year 2014 (≈ 3.145 million people)
Estimated mortality rate for recreational diving in the USA	~ 2 deaths per 100,000 participants per year	Indicative data of relatively low risk
Global participation growth trend	Average annual growth ~1.8% (recent five-year period)	Breakdown: "casual divers" +2.7% per year; slight decline among "core divers"

[18] Targher G., Byrne C. D., et al. (2021). *Nonalcoholic Fatty Liver Disease and Risk of Cardiovascular Disease: A Meta-analysis. Lancet Gastroenterol Hepatol.*, 6(11), 903–917.
[19] Kim D., et al. (2020). *Increased Risk of Cardiovascular Events in NAFLD: A Nationwide Cohort Study. Journal of Hepatology*, 73(5), 1062–1071.
[20] Lonardo A., et al. (2020). *NAFLD and Cardiovascular Disease: A Comprehensive Review. Journal of Internal Medicine*, 288(5), 402–421.
[21] Ballestri S., et al. (2017). *NAFLD as a Multisystem Disease: Insights from Clinical Practice. Hepatology*, 65(4), 1137–1154.

Table 1.2 – *Prevalence, geographical distribution, and estimated incidence of NAFLD in the adult population.* Source: Ballestri et al. (2017) and indexed literature (PMC)

Indicator	Value / description	Comments
Estimated global prevalence in the adult population	~ 32% (some meta-analyses) (PMC))	Based on global meta-analyses
European prevalence in adults	~ 26.9% (studies including 19 adults, 9 youths) (PMC)	Europe: men ~32.8%; women ~19.6% (PMC))
Variazioni regionali ("Africa", "Asia", "Sud America", "Medio Oriente")	Africa ~14%, Europe ~23%, USA ~24%, Asia ~27%, South America ~31%, Middle East ~32% (PMC))	Indicative data for large geographical areas
Estimated global incidence	~ 47 cases per 1,000 person-years (PMC)	Useful to show temporal evolution
Trend of increasing prevalence over time	Estimated prevalence increased from ~26% (pre-2005) to ~38% (post-2016) in studies (E-CMH)	Shows the increase of the condition over time

1. 5 Rationale for the convergence between recreational diving and NAFLD

The association between recreational diving activity and NAFLD, which is the focus of the present research project, is grounded in pathophysiological and preventive considerations. During a dive, the human body is exposed to significant environmental stressors — increased pressure, exposure to inert gases, temperature variations, microbubble formation, and endothelial and coagulative activation[22].

The adaptive response to these stressors requires an intact endothelium, efficient metabolism, and adequate vascular reserve. NAFLD, in contrast, is characterized by chronic low-grade systemic inflammation, endothelial dysfunction, and a pro-coagulant state, elements that may impair the organism's ability to manage the decompression phase[23]. These features make it plausible that NAFLD could represent a latent vulnerability factor for the development of DCS, particularly the

[22] Cialoni D., Pieri M., Marroni A. (2017). *Physiological Adaptations and Endothelial Response in Recreational Diving.Frontiers in Physiology*, 8, 1063.
[23] Xu R., Tao A., Zhang S., Chen G. (2024). *NAFLD and Endothelial Dysfunction: Mechanisms Linking Liver and Vascular Disease. Frontiers in Cardiovascular Medicine*, 11, 1378945.

"undeserved" forms, which account for approximately 60% of documented cases[24]. Should this correlation be confirmed, **the early identification of NAFLD in divers could open new preventive perspectives** by integrating hepatic and metabolic screening into dive fitness programs. From this standpoint, diving medicine could evolve toward a predictive and personalized model capable of combining operational safety with the promotion of metabolic health.

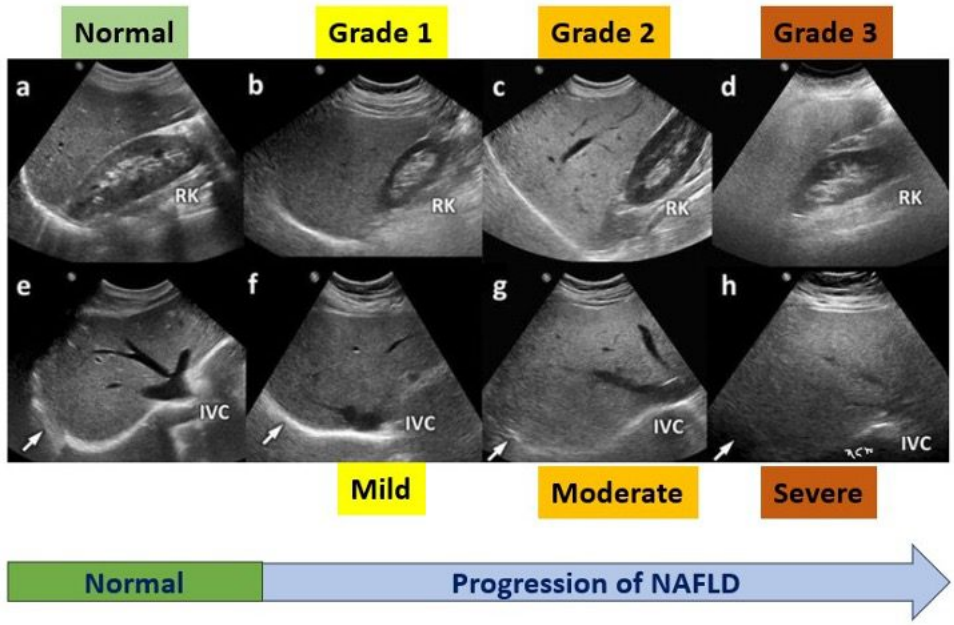

Figure 1.2 – *Ultrasound appearance of non-alcoholic fatty liver disease (NAFLD): diffuse increase in parenchymal echogenicity with posterior attenuation of the ultrasound beam.*
Source: POCUS.org, *Liver Ultrasound – Fatty Liver Disease,* 2025

[24] Vann R. D., et al. (2011). *Decompression Illness. Lancet*, 377(9760), 153–164.

1. 6 Clinical and morphological framework of decompression sickness: deserved and undeserved forms

Decompression sickness (DCS, or Patologie da Decompressione) comprises a set of clinical conditions characterized by the formation of inert gas bubbles within tissues and the bloodstream during or after ascent from a dive. From a clinical and morphological perspective, these manifestations can be classified into two groups:

1. **based on clinical presentation**, distinguishing between **type I and type II** forms;
2. based on the **anatomical localization** of symptoms.

In both cases, the distinction between "deserved" forms - associated with decompression profiles known to be at risk - and "undeserved" forms, arising despite strict compliance with procedures and tables, currently represents a crucial point in understanding the pathogenetic mechanisms and in assessing individual vulnerability.

1. 7 Clinical classification: Type I and II DCS/DCI

Type I DCS (cutaneous and osteoarticular) is considered the mildest and most peripheral form of the disease, predominantly affecting superficial and musculoskeletal tissues. The main manifestations include:

- **migratory joint pain**, particularly involving the shoulders, elbows, and knees ("the bends");
- **cutaneous manifestations** such as pruritus, erythema, cyanotic patches, or *cutis marmorata*;
- **localized subcutaneous edema**, less frequent but reported in the literature.

These forms generally tend to resolve completely with normobaric oxygen and hyperbaric chamber treatment, without permanent sequelae[25].

Type II DCS (neurological, vestibular, and pulmonary) represents a more severe, systemic, and often disabling form, involving vital organs or the nervous system. The most common symptoms include:

[25] Vann R.D., Butler F.K., Mitchell S.J., Moon R.E. *Decompression Illness. Lancet.* 2011;377(9760):153–164.

- **central or spinal neurological disturbances**, such as paresthesias, paresis, motor incoordination, and bladder dysfunction;
- **vestibular involvement**, with rotational vertigo, nystagmus, and postural instability, frequently associated with nausea and vomiting, even in the absence of decompression errors;
- **respiratory manifestations ("chokes")**, characterized by dyspnea, dry cough, retrosternal pain, and, in severe cases, cyanosis and reduced arterial oxygen saturation[26].

Although historically used for diagnostic and therapeutic purposes, this classification is currently integrated with imaging and biochemical assessments to achieve a more accurate definition of the systemic picture and the severity of tissue damage[27].

1. 8 Classification by anatomical district involved

In addition to the clinical distinction, it is useful to consider the anatomical localization of manifestations, which often helps to guide differential diagnosis and therapeutic choices.

- **Osteoarticular system** – intense and persistent joint pain predominates, often resembling inflammatory disorders. The most frequently involved joints are those subjected to biomechanical stress (shoulders, hips, and knees).
- **Skin and soft tissues** – *cutis marmorata* and localized pruritus represent early manifestations; in more severe cases, superficial ischemic necrosis (rare) may occur.
- **Central and peripheral nervous system** – paresthesias, motor deficits, incoordination, and sphincter disturbances are observed; in some cases, magnetic resonance imaging has revealed segmental spinal ischemic lesions correlated with symptom distribution[28].
- **Vestibular apparatus (often after scuba diving)** – rotational vertigo and nystagmus represent distinctive symptoms. Unlike the forms observed in deep breath-hold diving (*Taravana*), these manifestations do not result from acute pressure peaks but from circulating microbubbles or labyrinthine ischemia[29].

---

[26] Mitchell S.J. *Decompression Illness: A Comprehensive Overview. Diving and Hyperbaric Medicine.* 2024;54:1–53
[27] Cialoni D., Pieri M., Marroni A. *Endothelial Dysfunction and Decompression Sickness: Current Perspectives. Front Physiol.* 2017;8:1063.
[28] Brubakk A.O., Mollerløkken A., et al. *Bubble-Induced Endothelial Damage and Inflammation: Implications for Decompression Illness. J Appl Physiol.* 2003;94(6):2147–2153
[29] Edmonds C., Lowry C., Pennefather J. *Diving and Subaquatic Medicine.* 5th Ed. CRC Press; 2016.

1. 9 Clinical - morphological correlation between “deserved” and “undeserved” DCS

From a morphological standpoint, the two categories of DCS present similar tissue lesions - in particular microcirculatory damage, endothelial dysfunction, and inflammatory activation - but differ in the triggering mechanism.

In **“deserved” forms**, the damage is typically related to an overload of inert gas due to excessively deep dives or rapid ascents, resulting in massive bubble formation and acute ischemia.

“Undeserved” forms, by contrast, occur in the absence of decompression violations and appear to depend on individual predisposing conditions, such as:

- **chronic endothelial dysfunction**;
- **metabolic alterations** (insulin resistance, dyslipidemias);
- **chronic low-grade systemic inflammatory states**;
- **increased microcirculatory reactivity** and impaired pulmonary clearance of bubbles[30]-[31].

Morphological and histological studies conducted in animal models and on human ex vivo samples have demonstrated endothelial swelling, increased capillary permeability, activation of pro-inflammatory cytokines (TNF-α, IL-6, IL-8), and diffuse microthrombosis, regardless of the dive profile[32].

These findings strengthen the hypothesis that the biological vulnerability of the endothelium - rather than hyperbaric exposure alone - represents the key factor in the genesis of “undeserved” DCS, opening innovative perspectives in risk assessment and in the personalization of preventive strategies[33].

[30] Imbert J.P., Egi S.M., Germonpré P., Balestra C. *Static Metabolic Bubbles as Precursors of Vascular Gas Emboli During Divers' Decompression. Front Physiol.* 2019;10:807.
[31] Arieli R. *Nanobubbles Form at Active Hydrophobic Spots on the Luminal Aspect of Blood Vessels. Front Physiol.*2017;8:591.
[32] Carotti S., et al. *Liver Sinusoidal Endothelial Cells and Microvascular Dysfunction in NAFLD. Cells.* 2020;9(2):288.
[33] Balestra C., Germonpré P. *Towards a Personalized Decompression Approach. Front Physiol* 2021; 12:727324.

1. 10 Interpretative synthesis and pathophysiological perspective

The distinction between deserved and undeserved forms has not only descriptive value, but implies a paradigm shift in diving medicine: from the classical concept of technical error to an integrated model of individual biological risk. In this perspective, the assessment of metabolic profile, inflammatory status, and endothelial function may become an integral part of pre-dive screening protocols, promoting a predictive and personalized approach to diving medicine oriented toward prevention and the operational safety of the diver.

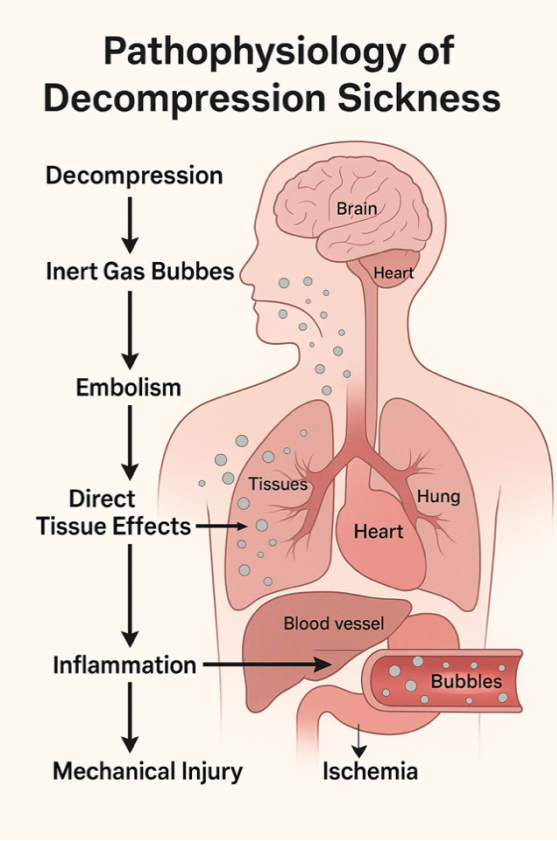

Figure 1.3 – *Pathophysiological scheme of decompression sickness.* Source: own elaboration (2025)

Methodological note

This chapter provides the epidemiological framework necessary for the development of the research hypothesis. The quantitative data and sources used (*PADI, DAN, AHA, PMC, BioMed Central*) were selected based on their scientific reliability and international representativeness[34]. In order to scientifically contextualize the hypothesis of this research project.

[34] DAN Europe & PADI Joint Report. (2023). *Global Diving Demographics and Safety Trends.* DAN-PADI Research Program.

Chapter 2 – Morphology and histology of hepatic tissue and vascular endothelium under physiological conditions

2. 1 Anatomical and physiological context of the chapter

A thorough understanding of the morphology and functional organization of the tissues involved in this research project - the vascular endothelium and hepatic tissue - is essential to correctly frame the pathophysiological hypotheses that will be developed in the following chapters.

In this section, the main histological and ultrastructural features of these compartments under physiological conditions are illustrated, with particular reference to the hepatic sinusoidal endothelium and the microenvironment of the hepatic lobule, where complex processes of exchange and metabolic regulation take place.

2. 2 Structure and function of the vascular endothelium under physiological conditions

The vascular endothelium represents a thin but dynamic cellular monolayer that lines the entire internal surface of the cardiovascular system, from the heart and large arterial vessels down to the capillaries.

Endothelial cells, of mesodermal origin, are typically flattened, elongated, and polarized along the axis of blood flow. Under physiological conditions, they do not merely play a passive lining role, but actively participate in the maintenance of vascular homeostasis by regulating vascular tone, the balance between coagulation and fibrinolysis, capillary permeability, and the inflammatory response.

From a structural perspective, the endothelium rests on a thin basement membrane composed of type IV collagen, laminin, and other glycoproteins that ensure cell adhesion and polarization. Intercellular junctions (tight, adherens, and gap junctions) guarantee the cohesion of the endothelial layer and modulate its permeability. On the luminal surface, caveolae, microvilli, and fenestrations are present, whose density varies according to the anatomical district, allowing selective exchanges with the interstitial compartment.

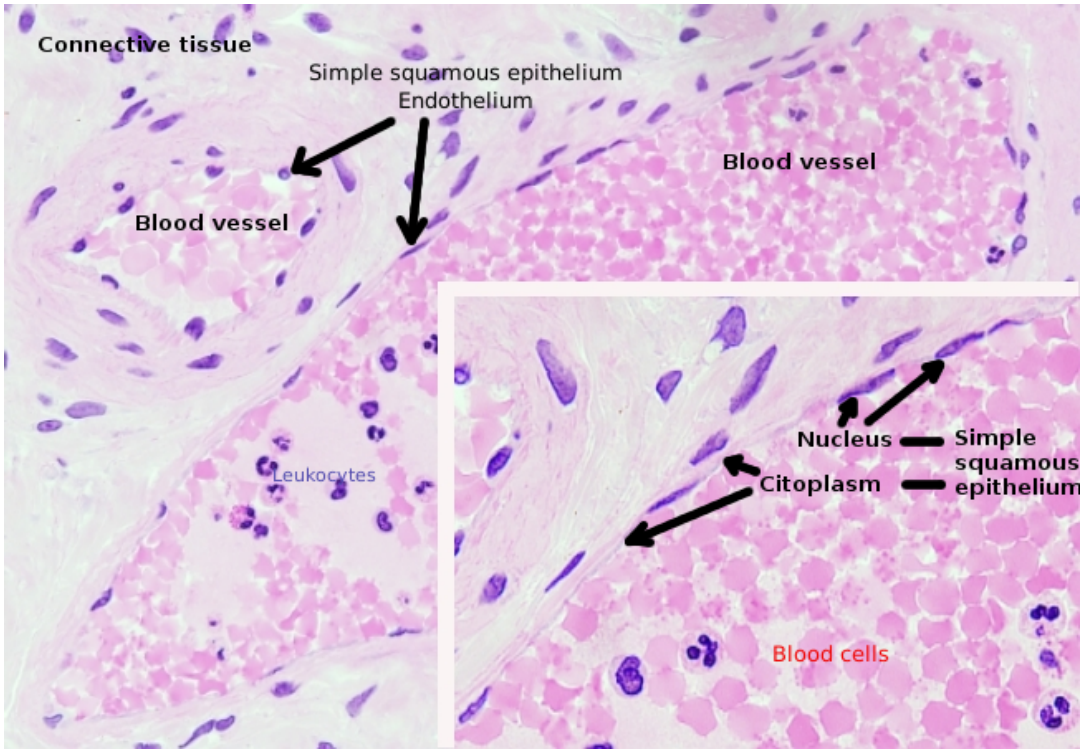

Figure 2.1 – *Vascular endothelium: a single layer of elongated squamous cells lining the inner surface of blood vessels.* Source: M. Megías, *Histology and Cell Biology – University of Vigo* (CC BY-NC-SA 4.0 license)

Based on morphology and permeability, the endothelium is classified into three main categories:

- **continuous**, as in the brain or skeletal muscle, where the endothelial barrier is almost impermeable;
- **fenestrated**, typical of the kidney, endocrine glands, and intestine, characterized by pores of 60–80 nm that facilitate the passage of small molecules;
- **sinusoidal or discontinuous**, present in the bone marrow, spleen, and, most notably, in the liver.

In the hepatic context, liver sinusoidal endothelial cells (LSEC) exhibit a highly specialized morphology: they possess numerous fenestrations of 50–150 nm, organized into “sieve plates,” and lack a continuous basement membrane.

This architecture enables efficient bidirectional exchange of molecules between portal blood and hepatocytes through the space of Disse. In addition to their filtering function, LSEC participate in hepatic immune regulation, the uptake of lipoproteins and hormones, and the modulation of

regenerative processes in the hepatic parenchyma. They also display high endocytic capacity and scavenger receptors, which contribute to the clearance of circulating macromolecules and debris[35]-[36].

The maintenance of endothelial integrity, particularly of the sinusoidal endothelium, represents a fundamental condition for normal liver physiology. Its alteration constitutes one of the earliest pathogenetic events in the transition toward dysfunctional states, such as hepatic steatosis and systemic vascular dysfunction.

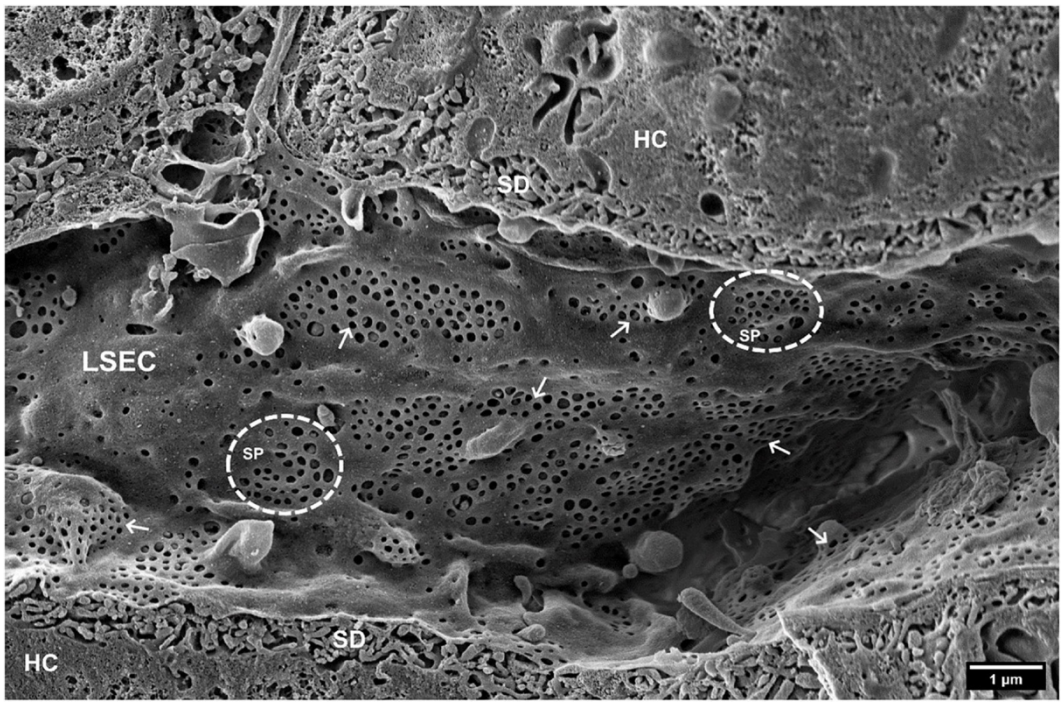

Figure 2.2 – *Hepatic sinusoidal endothelium (Liver Sinusoidal Endothelial Cells, LSEC) observed by scanning electron microscopy: the characteristic fenestrations enabling selective exchange between blood and the space of Disse are visible*. Source: adapted from Poisson J. et al., *Liver Sinusoidal Endothelial Cells: Physiology and Role in Liver Diseases*, Frontiers in Physiology, 2021 (12:735573), doi:10.3389/fphys.2021.735573.

[35] Carotti, S., Morini, S., Corradini, S. G., Burza, M. A., Molinaro, A., Carpino, G. (2020). *Liver Sinusoidal Endothelial Cells: Morphology, Function, and Role in Liver Diseases.* Cells, 9(3), 706.
[36] Géraud, C., Evdokimov, K., Straub, B. K., Peitsch, W. K., Demory, A., Denecke, B., et al. (2012). *Unique cell type-specific junctional complex architecture of liver sinusoidal endothelial cells.* Journal of Hepatology, 57(4), 736–749.

2. 3 Anatomy and histology of healthy hepatic tissue

The liver, a parenchymal organ of endodermal origin, is organized into functional units known as hepatic lobules. Each lobule presents a central vein in the center and, at the periphery, the portal triads, composed of a branch of the portal vein, a branch of the hepatic artery, and an interlobular bile duct. Blood flow moves from the periphery toward the center through the hepatic sinusoids, irregular and anastomosing vascular channels that create a unique hemodynamic and biochemical microenvironment.

The sinusoids, lined by LSEC, are in close contact with hepatocytes through the space of Disse, a thin compartment interposed between the endothelium and the basolateral membrane of hepatocytes.

Within this space reside Ito cells (or stellate cells), which store vitamin A and play a central role in fibrogenesis in response to injury. In parallel, Kupffer cells, the resident macrophages of the liver, are distributed along the sinusoids and participate in immune surveillance and the phagocytosis of blood-borne debris.

Hepatocytes, large polyhedral cells, account for approximately 80% of the hepatic cellular mass. They are generally mono- or binucleated, with eosinophilic cytoplasm rich in mitochondria, smooth and rough endoplasmic reticulum, and a well-developed Golgi apparatus, reflecting intense biosynthetic activity.

Functional polarization is marked:

- **the basolateral membrane**, facing the space of Disse, is equipped with microvilli for nutrient absorption;
- **the apical membrane** delineates the bile canaliculi, the site of bile secretion.

From a metabolic standpoint, the hepatic lobule exhibits a clear porto-central zonation. Periportal cells (zone 1) are predominantly involved in gluconeogenesis, β-oxidation, and amino acid metabolism, whereas perivenular cells (zone 3) perform functions related to glycolysis, lipogenesis, and cytochrome P450-mediated detoxification[37]-[38]. This compartmentalization renders specific

[37] Cotoi, C., & Quaglia, A. (2016). *Histopathological aspects of liver regeneration and zonation.* Hepatology Research, 46(10), 895–907.
[38] Guido, M., Sarcognato, S., & Sacchi, D. (2019). *Histology of the normal liver.* In: De Groote, J., & Brunt, E. (eds.), *Liver Pathology*. Springer.

regions of the lobule more vulnerable to particular insults: for example, zone 3 is more susceptible to hypoxia, whereas zone 1 is more affected by excess metabolic substrates.

In homeostatic conditions, the healthy liver displays a remarkable regenerative capacity, supported by continuous crosstalk between parenchymal cells (hepatocytes) and non-parenchymal cells (endothelial cells, Kupffer cells, and stellate cells). This cellular synergy is essential for growth, tissue repair, and the response to harmful stimuli.

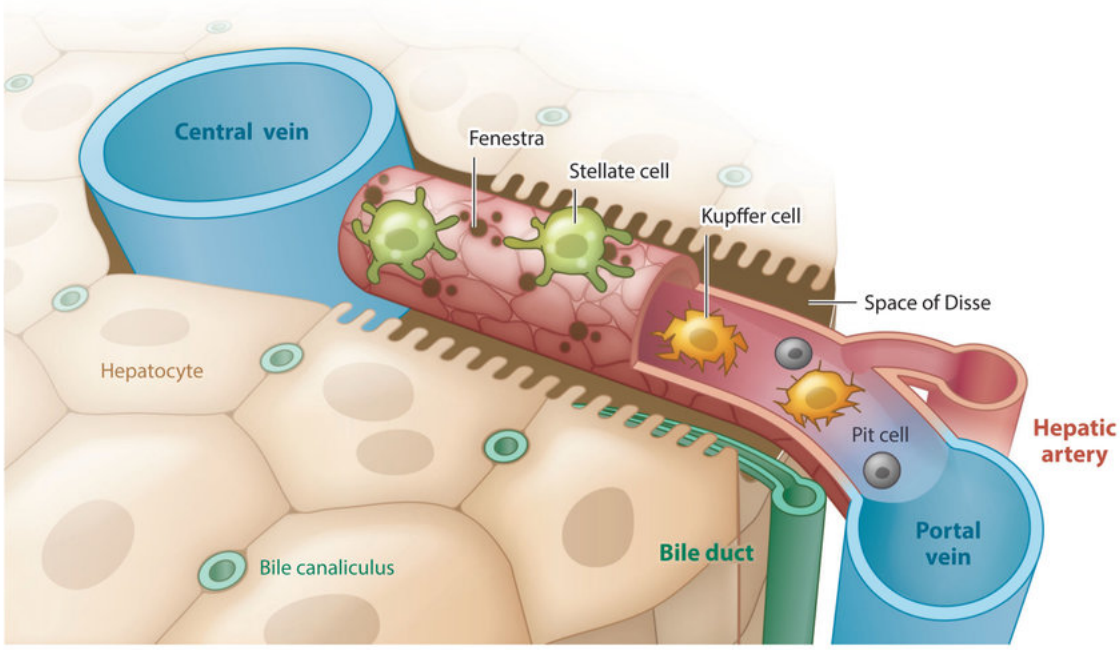

Figure 2.3 – *Schematic representation of the hepatic sinusoid: the fenestrated sinusoidal endothelium allows the passage of molecules between the blood and hepatocytes through the space of Disse; Kupffer cells and hepatic stellate cells (Ito cells) are also visible.* Source: adapted from Sørensen K.K. et al., *The Scavenger Cells of the Liver – The Liver Sinusoidal Endothelial Cell and the Kupffer Cell*, Frontiers in Physiology, 2019 (10:1032), doi:10.3389/fphys.2019.01032. CC BY 4.0 license.

Chapter 3 – Morphological and histological alterations of the hepatocyte and hepatic tissue in non-alcoholic fatty liver disease (NAFLD)

3. 1 General framework and objectives of the chapter

Non-alcoholic fatty liver disease (NAFLD) represents one of the most frequent pathological conditions of the liver in Western countries and constitutes the initial stage of a progressive clinical spectrum that includes non-alcoholic steatohepatitis (NASH), fibrosis, cirrhosis, and, in advanced stages, hepatocellular carcinoma (HCC) [39]. In this section, the morphological and ultrastructural modifications that characterize the transformation of the healthy hepatocyte into a steatotic hepatocyte are analyzed, with an integrated anatomic-pathological perspective aimed at understanding the correlation between lipid accumulation, subcellular damage, and tissue dysfunction.

3. 2 Morphological and histological aspects of the steatotic hepatocyte

The steatotic hepatocyte is characterized by the intracellular accumulation of neutral lipids, predominantly triglycerides, which are deposited in the form of lipid vacuoles of variable size within the cytoplasm. This process, reversible in the early stages, is determined by a metabolic imbalance between the hepatic uptake, synthesis, oxidation, and secretion of fatty acids[40].

From a histological perspective, two main forms of steatosis are distinguished:

- **Macrovesicular steatosis**, in which the cytoplasm is occupied by a single large lipid droplet that displaces the nucleus toward the cell periphery. This is the most common form in NAFLD and predominantly affects the centrilobular zone (zone 3) of the hepatic lobule, where oxidative capacity

[39] Takahashi, Y., & Fukusato, T. (2014). *Histopathology of Nonalcoholic Fatty Liver Disease.* World Journal of Gastroenterology, 20(42), 15539–15548.

[40] Sanyal, A. J., Campbell-Sargent, C., Mirshahi, F., et al. (2001). *Nonalcoholic Steatohepatitis: Association of Insulin Resistance and Mitochondrial Abnormalities.* Gastroenterology, 120(5), 1183–1192.

is lower and vulnerability to metabolic damage is greater[41]. At these initial stages, the lobular architecture is still preserved, but cytoplasmic ballooning and nuclear compression represent early signs of dysfunction.

• **Microvesicular steatosis**, less frequent, characterized by the presence of numerous small lipid droplets that do not displace the nucleus, giving the hepatocyte a "foamy" appearance. This form is generally associated with severe mitochondrial damage and is more commonly observed in acute conditions (e.g., Reye's syndrome or drug-induced hepatotoxicity), but it may coexist with macrovesicular steatosis in advanced NAFLD[42].

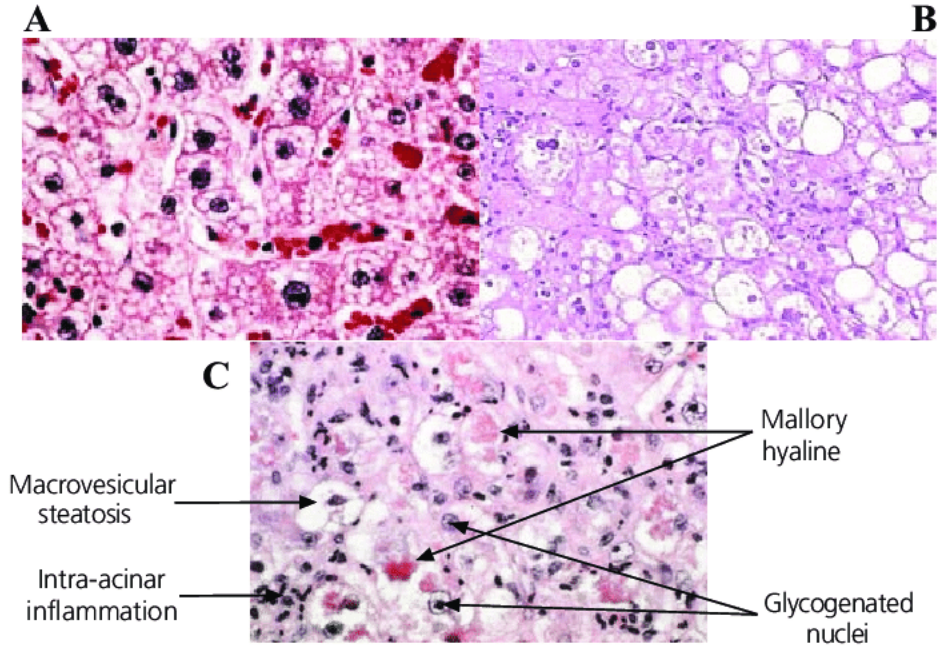

Figure 3.1 – *Comparison between microvesicular (A) and macrovesicular (B) hepatic steatosis. In the microvesicular form, hepatocytes show numerous small lipid vacuoles, with a central nucleus and finely granular cytoplasm; in the macrovesicular form, the single large lipid droplet displaces the nucleus to the periphery of the cell.* Source: adapted from Younossi Z.M. et al., *Histopathology of Non-alcoholic Fatty Liver Disease and Steatohepatitis*, World Journal of Gastroenterology, 2014; 20(42):15019–15029.

[41] Brunt, E. M., Kleiner, D. E., Wilson, L. A., et al. (2022). *NAFLD and NASH Pathology: An Update.* Hepatology, 76(6), 1880–1893.
[42] Tandra, S., Yeh, M. M., Brunt, E. M. (2011). *Pathology of Nonalcoholic Fatty Liver Disease: An Overview.* Clinics in Liver Disease, 15(1), 11–26.

In addition to lipid deposition, the steatotic hepatocyte exhibits significant ultrastructural alterations:

- cytoplasmic ballooning and disorganization of microfilaments;
- hypertrophy of the smooth endoplasmic reticulum and lysosomal vacuolization;
- mitochondrial alterations, with loss of cristae and reduced β-oxidation;
- reduction of cellular polarity, with disorientation of bile canaliculi.

These features represent early markers of subcellular damage, which precede the transition toward steatohepatitis (NASH), in which lobular inflammation, apoptosis, and initial fibrogenic processes are associated[43]. The lobular microenvironment also undergoes structural modifications: the space of Disse tends to narrow, stellate cells (Ito cells) become activated toward a myofibroblastic phenotype, and liver sinusoidal endothelial cells (LSEC) lose their fenestrations, a phenomenon that contributes to increased intrahepatic vascular resistance and microcirculatory dysfunction[44].

Thus, hepatic steatosis is not simply a passive accumulation of fat, but a dynamic and multifactorial process with direct repercussions on the metabolic and vascular function of the entire liver.

3. 3 Histological classification and grading of hepatic steatosis

The histological assessment of NAFLD is performed using conventional staining techniques (hematoxylin–eosin, Sudan, Oil Red O on cryostat sections) and follows standardized semi-quantitative criteria. The most widely used system is the NAFLD Activity Score (NAS), proposed by the NASH Clinical Research Network, which integrates three fundamental components:

1. **Steatosis** (quantification of lipid deposition);
2. **Cytoplasmic ballooning**;
3. **Lobular inflammation[45]**.

[43] Farrell, G. C., van Rooyen, D., Gan, L., Chitturi, S. (2012). *NASH is an Inflammatory Disorder: Pathogenic, Prognostic and Therapeutic Implications.* Gut Liver, 6(2), 149–171.
[44] Poisson, J., Lemoinne, S., Boulanger, C., et al. (2017). *Liver Sinusoidal Endothelial Cells: Physiology and Role in Liver Diseases.* Journal of Hepatology, 66(1), 212–227.
[45] Kleiner, D. E., Brunt, E. M., Van Natta, M., et al. (2005). *Design and Validation of a Histological Scoring System for NAFLD.* Hepatology, 41(6), 1313–1321.

The specific grading of steatosis is based on the percentage of hepatocytes involved, regardless of the type of accumulation (micro- or macrovesicular), according to the following scale:

Table 3.1- Histological grading of hepatic steatosis based on the extent of hepatocyte involvement. Source: adapted from Brunt et al., *Nonalcoholic fatty liver disease: histopathologic features and clinical correlations*, Hepatology, 1999, and subsequent revisions.

Grade	Percentage of hepatocytes involved	Main histological features
0 – Absent	< 5%	Hepatocytes with clear cytoplasm, absence of lipid vacuoles.
1 – Mild	5–33%	Scattered lipid vacuoles, predominantly in zone 3; preserved lobular architecture.
2 – Moderate	34–66%	More homogeneous distribution, extension to zone 2 and periportal areas, moderate architectural distortion.
3 – Severe	> 66%	Pan-lobular involvement, cytoplasmic compression, alteration of the sinusoid–hepatocyte ratio, possible associated inflammation.

The table reports the standard histological classification of hepatic steatosis, articulated into four grades (0–3) based on the percentage of hepatocytes involved and the main morphological features observable under light microscopy.

There is no grade 4 in the standard classification, as such a condition would imply massive hepatocellular damage no longer attributable to pure steatosis, but rather to subsequent evolutionary stages (steatohepatitis, fibrosis, or cirrhosis). Some experimental proposals introduce descriptive categories beyond grade 3 to indicate extensive pan-lobular patterns, but these variants are not officially recognized in international grading systems[46].

[46] Brunt, E. M., et al. (2022). *NAFLD and NASH Pathology: An Update.* Hepatology, 76(6), 1880–1893.

Chapter 4 - Ultrasound diagnostic aspects of NAFLD

4. 1 Complementary techniques and diagnostic innovations in the ultrasound assessment of NAFLD

In recent years, hepatic ultrasound has undergone a significant technological evolution, shifting from a purely qualitative evaluation to a semiquantitative and integrated approach capable of providing not only morphological but also functional and biophysical information on the hepatic parenchyma[47].

In both clinical and research settings, this transformation has improved data reproducibility, diagnostic sensitivity in mild forms, and correlation with histological parameters, traditionally considered the gold standard reference[48].

Among the main diagnostic innovations, two methods deserve particular attention:

1. **ultrasound steatometry** using the hepato-renal index (HRI);
2. **controlled attenuation parameter (CAP)** technology integrated into transient or multifrequency elastography devices[49]-[50].

4. 2 Hepato-renal index (HRI) and quantification of steatosis

The HRI enables a quantitative assessment of the echogenicity ratio between the liver and the kidney, calculated through homogeneous regions of interest (ROI) acquired under standardized technical conditions.

An HRI value greater than 1.5 is generally considered indicative of significant hepatic steatosis, whereas values above 2.0 are associated with severe steatosis, with a specificity exceeding 85%[51].

---

[47] Khov N., Sharma A., Riley T. (2014). *Bedside Ultrasound in the Diagnosis of Nonalcoholic Fatty Liver Disease.World Journal of Gastroenterology*, 20(22), 6821–6825.
[48] Bril F., Ortiz-Lopez C., Lomonaco R., et al. (2015). *Clinical Value of Liver Ultrasound for the Diagnosis of Nonalcoholic Fatty Liver Disease in Overweight and Obese Patients. Liver International*, 35(9), 2139–2146.
[49] Venidiktova D., Borsukov A., Alipenkova A. V., et al. (2019). *Ultrasound Steatometry in Patients with Nonalcoholic Fatty Liver Disease: Pilot Results. Journal of Clinical Practice*, 10(1), 23–29.
[50] Benjamin A., Zubajlo R., Thomenius K., et al. (2017). *Non-Invasive Diagnosis of Non-Alcoholic Fatty Liver Disease Using Ultrasound Image Echogenicity. IEEE Engineering in Medicine and Biology Conference*, 2920–2923
[51] Webb M., Yeshua H., Zelber-Sagi S., et al. (2009). *Diagnostic Value of a Computerized Hepato-Renal Index for Quantitative Evaluation of Fatty Liver. Journal of Hepatology*, 51(6), 1069–1076.

Compared with simple visual assessment, this method offers an advantage in terms of **objectivity**, reducing inter- and intra-observer variability. However, it requires careful calibration of ultrasound gain settings and an experienced operator to ensure reliable results.

4. 3 Controlled attenuation parameter (CAP) and elastographic integration

The CAP parameter, introduced as an extension of FibroScan® technology, measures the attenuation of the ultrasound beam as it passes through the hepatic parenchyma. This attenuation is proportional to intracellular lipid content and allows a quantitative estimation of steatosis that is independent of the operator[52].

CAP values are expressed in decibels per meter (dB/m), and thresholds of 248–288 dB/m are considered predictive of steatosis ≥ S1, whereas values above 300 dB/m are associated with advanced steatosis (≥ S2) [53]. The combination of CAP with the measurement of liver stiffness (kPa) enables the simultaneous assessment of steatosis and fibrosis, improving diagnostic accuracy and providing a multiparametric characterization of the liver[54].

4.3.1 Quantitative ultrasound and advanced steatometry

The introduction of quantitative ultrasound (QUS) systems and techniques based on backscatter coefficient (BSC) and speed of sound (SoS) represents a further step toward the digital diagnosis of NAFLD. These tools analyze acoustic reflection at the microstructural level, enabling a numerical estimation of hepatic lipid content with high reproducibility and without the need for contrast agents. Early comparative studies between QUS and MRI-PDFF (Proton Density Fat Fraction) have shown

[52] Sasso M., Beaugrand M., de Ledinghen V., et al. (2010). *Controlled Attenuation Parameter (CAP): A Novel Tool for the Non-Invasive Evaluation of Steatosis Using FibroScan®. Journal of Hepatology*, 53(6), 1030–1037.
[53] Eddowes P. J., Sasso M., Allison M., et al. (2019). *Accuracy of FibroScan Controlled Attenuation Parameter (CAP) and Liver Stiffness Measurement in Assessing Steatosis and Fibrosis in NAFLD. Gastroenterology*, 156(6), 1717–1730.
[54] Caussy C., Reeder S. B., Sirlin C. B., Loomba R. (2018). *Non-Invasive Quantitative Assessment of Liver Fat by Ultrasound and Magnetic Resonance Imaging. Nature Reviews Gastroenterology & Hepatology*, 15(10), 627–644.

a correlation greater than 0.85, indicating the potential of this technology as a cost-effective and non-invasive alternative to magnetic resonance imaging[55]-[56].

4.3.2 Methodological considerations and future perspectives

In the context of the present research, the use of advanced ultrasound techniques provides a quantitative and standardizable basis for the assessment of hepatic steatosis in the divers involved in the study.

The integration of morphological parameters (classical ultrasound patterns) and quantitative metrics (HRI, CAP, elastography) allows for a more precise and comparable diagnosis, useful both for clinical purposes and for correlation with molecular and pathophysiological data obtained in vitro and in vivo.

In the future, the fusion of conventional ultrasound with artificial intelligence (AI-based steatosis mapping) represents a promising direction for the early diagnosis and risk stratification of NAFLD, with potential applications also in personalized diving medicine, where the assessment of metabolic and hepatic profiles could become an integral part of dive fitness protocols[57].

[55] Lee D. H., Lee J. Y., Bae J. S., et al. (2020). *Quantitative Ultrasound Using Backscatter Coefficient for the Evaluation of Hepatic Steatosis: A Prospective Study. Ultrasound in Medicine & Biology*, 46(7), 1776–1785.
[56] Dioguardi Burgio M., Ronot M., Reizine E., et al. (2023). *Emerging Role of Quantitative Ultrasound in Liver Steatosis Assessment: From Physics to Clinical Application. European Radiology*, 33(8), 5746–5760.
[57] Piscaglia F., et al. (2022). *Artificial Intelligence in Liver Ultrasound: Current Evidence and Future Perspectives. Journal of Hepatology*, 77(6), 1682–1695.

Chapter 5 – Pathophysiological and morphological aspects of bubble formation during scuba diving

5. 1 General framework of decompression pathophysiology

Despite significant advances in diving safety due to the introduction of standardized decompression tables and conservative ascent algorithms, the formation of intravascular and/or tissue gas bubbles (*Vascular Gas Emboli*, VGE) remains the main pathophysiological mechanism underlying decompression sickness (DCS) [58].

The phenomenon does not depend solely on the amount of gas dissolved in the tissues, but primarily on the way in which these gases - mainly nitrogen - return to the gaseous phase during ascent, when ambient pressure decreases at the end of the dive.

Under physiological conditions, nitrogen is gradually eliminated through pulmonary respiration during ascent. However, in the presence of tissue supersaturation - that is, when the partial pressure of the dissolved gas exceeds ambient pressure - a phase transition may occur with the formation of microbubbles or macrobubbles. The appearance and dynamics of these bubbles depend not only on the dive profile and ascent rate, but also on a complex series of individual biological factors, including the state of the vascular endothelium, the presence of micronuclei or cavitation nuclei, and predisposing metabolic conditions[59].

---

[58] Arieli, R. (2019a). *Decompression Bubbles: Pathophysiology and Clinical Relevance.* Diving and Hyperbaric Medicine, 49(3), 137–144.

[59] Mitchell, S. J., & Doolette, D. J. (2013). *Pathophysiology of Decompression Sickness.* Comprehensive Physiology, 3(3), 1633–1670.

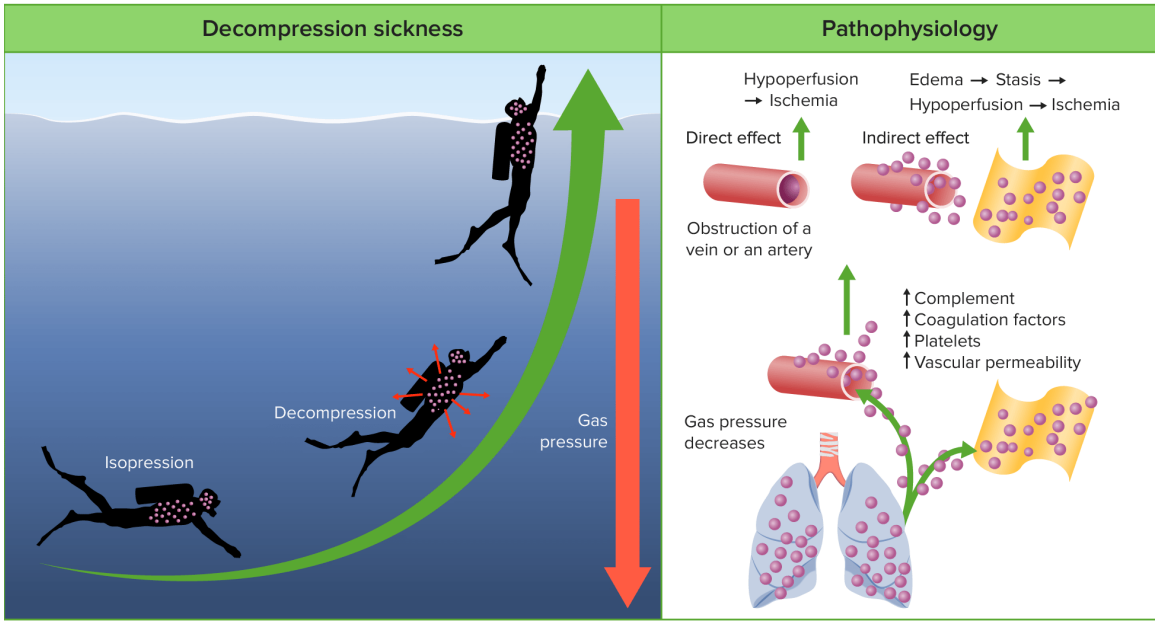

Figure 5.1 – *Illustrative diagram of the pathogenesis of decompression sickness (Decompression Sickness).* Source: adapted from Lecturio Medical Education – *Decompression Sickness (DCS)*, 2023

5. 2 Micronuclei and "Active Hydrophobic Spots" (AHS)

The currently most accepted model to explain the origin of pathological bubbles is based on the existence of pre-existing gaseous micronuclei within the vascular system. These small submicroscopic aggregates - not detectable with conventional imaging techniques - act as nucleation sites around which dissolved gas molecules aggregate, forming macroscopic bubbles during the desaturation phase[60].

According to Arieli's model, the formation of micronuclei is favored by the presence of "Active Hydrophobic Spots" (AHS), that is, hydrophobic microdomains (e.g., lipids) on the endothelial surface where thermodynamically favorable conditions for gas aggregation are created[61]. These spots may originate from lipid or structural alterations of the endothelial membrane, such as the exposure of phospholipids or denatured proteins.

Some experimental evidence suggests that chronic metabolic disorders - including obesity, dyslipidemia, and metabolic syndrome - may increase the density and activation of AHS, thereby

[60] Vann, R. D., Butler, F. K., Mitchell, S. J., Moon, R. E. (2011). *Decompression Illness.* Lancet, 377(9760), 153–164.
[61] Arieli, R. (2017). *The Physicochemical Mechanisms of Bubble Formation in Diving.* Journal of Applied Physiology, 122(2), 385–392.

facilitating gas bubble nucleation and growth[62]. This makes it plausible that metabolically driven endothelial dysfunction represents a biological vulnerability factor in the pathogenesis of DCS, even in the absence of technical errors during the dive. To date, NAFLD has not yet been investigated as a dysfunction that could enhance the development of AHS.

5. 3 Systemic pathophysiology of the bubble

Once formed, a gas bubble can exert mechanical and biological effects on the vascular system.

From a mechanical standpoint, the bubble may partially or completely obstruct the lumen of small vessels, causing embolization, local ischemia, and tissue hypoxia. From a **biological** perspective, the direct interaction between the bubble surface and the vascular endothelium triggers an inflammatory cascade, with:

- activation of pro-inflammatory cytokines;
- leukocyte adhesion and release of pro-coagulant mediators;
- increased endothelial permeability and vasomotor dysfunction[63].

These processes amplify the initial tissue damage and may lead to multiorgan dysfunction in severe cases of systemic DCS.

In the presence of anatomical shunts - such as a patent foramen ovale (PFO) or intrapulmonary shunts - venous bubbles may pass into the arterial circulation, generating paradoxical embolism responsible for severe neurological and vestibular forms of DCS[64]. The concomitance of endothelial alterations and metabolic factors (e.g., diabetes) may further exacerbate the systemic inflammatory and pro-thrombotic response.

---

[62] Imbert, J. P., Cialoni, D., Sponsiello, N., et al. (2019). *Obesity and Metabolic Disorders as Risk Modifiers for Decompression Stress.* Frontiers in Physiology, 10, 1453.
[63] Currens, M. A., Moon, R. E., Freiberger, J. J. (2025). *Inflammatory Cascade Activation by Intravascular Gas Bubbles.* Undersea and Hyperbaric Medicine, 52(1), 23–34.
[64] Cialoni, D., Pieri, M., Marroni, A., et al. (2017). *The Role of Patent Foramen Ovale and Pulmonary Shunts in Diving Decompression Illness.* European Journal of Applied Physiology, 117(11), 2129–2140.

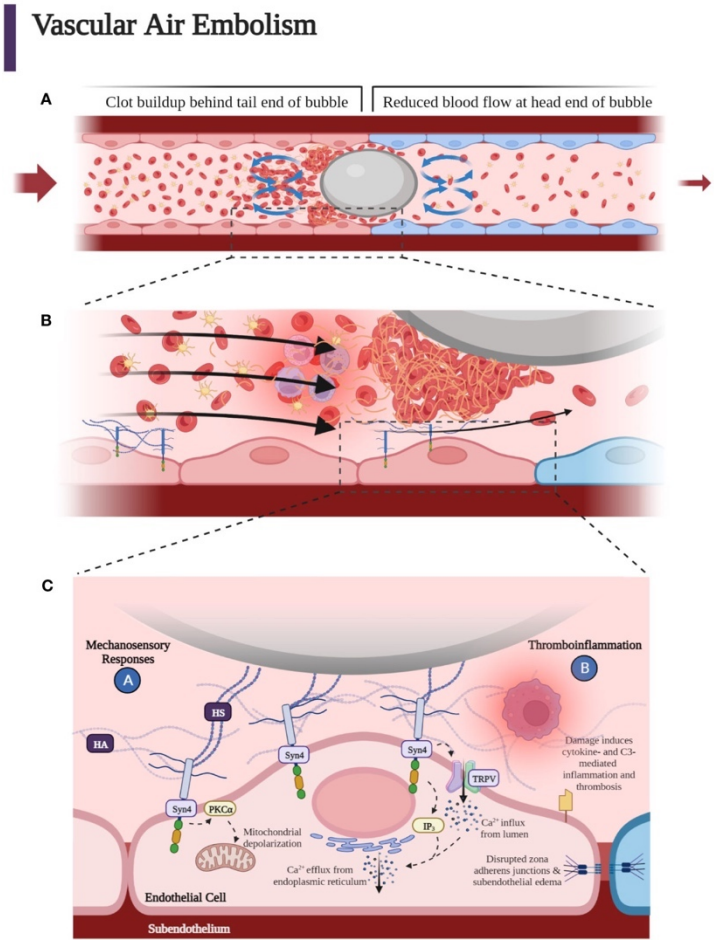

Figure 5.2 – *Interaction between intravascular gas bubbles and the vascular endothelium.* Source: adapted from Thom S. R. et al., *Frontiers in Immunology*, 2023, 14:1230049. DOI: *10.3389/fimmu.2023.1230049*

5. 4 Individual variability in bubble production

It is well documented that the amount of VGE detectable after a dive varies considerably from one individual to another, even under identical dive profiles[65]. This variability depends on genetic, epigenetic, and metabolic factors that influence:

- the density of pre-existing micronuclei;
- endothelial reactivity;
- endogenous antioxidant capacity and vascular elasticity.

[65] Lambrechts, K., Germonpré, P., Balestra, C. (2017). *Individual Variability in Decompression Bubble Formation: Physiological and Biochemical Perspectives.* Diving and Hyperbaric Medicine, 47(4), 204–210

In particular, individuals with type 2 diabetes or dyslipidemia often exhibit chronic endothelial dysfunction, with altered nitric oxide (NO) production and increased leukocyte adhesiveness, conditions that may promote both bubble formation and adhesion to the vascular wall[66].

Similarly, advanced age, physical inactivity, and visceral fat accumulation increase tissue solubility of nitrogen, modifying the saturation and desaturation kinetics of body compartments[67]. These physiological differences help explain why, even when safe diving protocols are followed, some individuals develop "undeserved" DCS while others remain asymptomatic.

5. 5 Key points for the research project

Gas bubble formation during scuba diving represents a complex and multifactorial phenomenon, determined by the interaction between mechanical variables (dive profile, ascent times) and biological variables (endothelial integrity, metabolism, inflammation). The growing evidence that metabolic conditions can alter endothelial microstructure and promote gas nucleation suggests a pathophysiological rationale for considering **cardiometabolic diseases** as potential risk factors in undeserved DCS.

[66] Arya, A., Patel, N., Mistry, S., et al. (2023). *Endothelial Dysfunction and Metabolic Syndrome: Implications for Vascular Gas Emboli Formation.* Journal of Applied Physiology, 135(1), 12–24.
[67] Lambrechts, K., Balestra, C., Germonpré, P. (2017). *Physical Fitness, Nitrogen Solubility and Decompression Stress.* Diving and Hyperbaric Medicine, 47(4), 202–208.

Chapter 6 – Experimental section

6. 1 In vitro experimental models and pathophysiological rationale

To systematically investigate the possible correlation between non-alcoholic fatty liver disease (NAFLD) and "undeserved" decompression sickness in divers, the doctoral project was structured into two complementary lines of research, developed in parallel over the three years of the PhD program.

The first line, of an **in vitro experimental** nature, was conducted on hepatic cell lines (HEPG2), with the aim of reproducing and characterizing in the laboratory a controlled model of hepatic steatosis to be used for immunohistochemical studies. This procedure made it possible to obtain in vitro cellular samples suitable for immunohistochemical evaluations and molecular assays, aimed at identifying pro-inflammatory mediators and patterns of endothelial damage potentially involved in the pathophysiological mechanisms of vulnerability and in the triggers of gas bubble formation risk, and therefore of decompression sickness. Primarily, a critical analysis of recent literature was carried out regarding techniques for inducing steatosis in hepatic cell cultures, as well as the main mediators to be investigated (pro-inflammatory and pro-coagulant cytokines and interleukins) and the most appropriate detection methods to ensure an objective and reproducible assessment of this part of the study.

The second part of the project, of an **in vivo nature**, involved the investigation of divers through preliminary hepatic ultrasound studies aimed at identifying, among participants, the presence or absence and any degree of non-alcoholic hepatic steatosis. Subsequently, all subjects, both with and without steatosis, were subjected to a controlled dry dive in a hyperbaric chamber (a therapeutic medical device used in healthcare to significantly increase the amount of gas dissolved in blood, fluids, and tissues to treat various pathological conditions such as carbon monoxide (CO) poisoning, osteomyelitis, aseptic bone necrosis, and delayed healing of difficult wounds); the hyperbaric chamber allows ambient pressures to be increased, thus simulating the same physical conditions that occur in the body during an underwater dive. In order to standardize the dive profile for all participants, reduce bias, enhance safety for the tested subjects, and ultimately better observe post-dive adaptive and physiological responses and compare them between subjects with and without NAFLD, the experimental tests underlying the doctoral project were conducted in a hyperbaric chamber rather than in water.

This chapter is primarily devoted to the in vitro phase, which constitutes the preliminary experimental basis of the doctoral project and represents the histological premise for the interpretation of results and for subsequent biological and biochemical evaluations.

6.1.1 In vitro models for the reproduction of hepatic steatosis: cell lines, approaches, and experimental rationale

The experimental reproduction of non-alcoholic fatty liver disease (NAFLD) *in vitro* represents a well-established strategy to investigate the cellular and molecular mechanisms underlying pathological lipid accumulation in hepatocytes[68].

Among the hepatic cell lines most commonly used in experimental steatosis models are HepG2 cells, epithelial lines derived from human hepatocellular carcinoma, which, although not fully replicating the functional complexity of primary hepatocytes (particularly with regard to insulin response and lipid metabolism), offer several experimental advantages: they are manageable, stable over time, easily cultivable long term, and capable of accumulating cytoplasmic lipid droplets in response to steatogenic stimuli, thereby mimicking the steatotic phenotype typical of NAFLD[69].

In vitro steatosis induction is generally achieved by exposing cells to mixtures of free fatty acids (FFA), mainly a combination of oleic acid (C18:1) and palmitic acid (C16:0), solubilized in bovine serum albumin (BSA) and administered at concentrations ranging from 0.25 mM to 1.5 mM for periods varying between 24 and 72 hours[70].

It has been demonstrated that a 2:1 ratio between oleate and palmitate induces optimal lipid accumulation, effectively reproducing the steatotic condition without causing significant cellular toxicity. This is the ratio that we used in our laboratory for our latest HepG2 cells.

The degree of intracellular lipid accumulation can be monitored using specific stains (Oil Red O, Nile Red, BODIPY) and subsequently quantified by spectrophotometry, confocal imaging, or fluorimetric assays. At the transcriptional and biochemical level, steatotic models show increased expression of

---

[68] Luangmonkong, T., et al. (2023). *High-Content Assay for Tuning Mitochondrial Function in NAFLD Models.*Archives of Toxicology, 97(3), 823–835.
[69] Papackova, Z., et al. (2015). *Selective Insulin Resistance in Human Steatotic HepG2 Cells.* BMC Gastroenterology, 15, 114.
[70] Luangmonkong, T., et al. (2023). *High-Content Assay for Tuning Mitochondrial Function in NAFLD Models.*Archives of Toxicology, 97(3), 823–835.

key lipogenic genes (SREBP-1c, PPARγ) and fatty acid uptake genes (CD36), accompanied by reduced expression of genes involved in lipoprotein secretion and insulin response, such as *GLUT2, PON1, and CEACAM1*[71].

In parallel, steatotic cells exhibit marked mitochondrial dysfunction and increased production of reactive oxygen species (ROS), conditions that foster a pro-inflammatory and pro-coagulant microenvironment[72]. These alterations are of particular interest in the context of the present project, as they represent predisposing conditions common to the mechanisms of endothelial vulnerability and gas bubble formation described in the pathophysiology of decompression sickness (DCS) at the tissue level.

6.1.2 IL-6 production in the cellular model of induced hepatic steatosis

In the experimental model of induced hepatic steatosis on HepG2 cells, the production of the pro-inflammatory cytokine interleukin-6 (IL-6) was assessed as an early indicator of cellular inflammatory activation and alteration of the hepatocellular microenvironment.

As shown in Figure 5.1, control cells display relatively low basal levels of IL-6, consistent with a non-steatotic metabolic state. In contrast, cells subjected to steatogenic induction (samples S1 and S2) show a **marked and consistent increase in IL-6 production**, with values clearly higher than those of the control. The increase is already evident in sample S1 and remains elevated in sample S2, suggesting a stable and reproducible inflammatory response associated with intracellular lipid accumulation.

This increase in IL-6 production is consistent with findings reported in the literature for in vitro NAFLD models, in which the accumulation of free fatty acids in hepatocytes triggers inflammatory pathways, oxidative stress, and mitochondrial dysfunction, leading to the release of pro-inflammatory mediators. In this context, IL-6 represents a key cytokine not only in the modulation of the local inflammatory response, **but also in liver–endothelium systemic communication**.

---

[71] Jin, R., et al. (2020). *Annexin A2 Indicates Hepatic Insulin Resistance and Steatosis in NAFLD.* Metabolism, 107, 154234.
[72] Parmar, S. R., et al. (2023). *Oxidative Stress-Mediated Liver Injury in Steatosis: Mechanistic Insights and Therapeutic Approaches.* Frontiers in Pharmacology, 14, 1122457.

From a pathophysiological standpoint, the increased IL-6 production observed in the steatotic model is particularly relevant for the present doctoral project. **IL-6 is indeed involved in endothelial dysfunction, activation of the coagulation cascade, and modulation of vascular permeability, all elements recognized as predisposing factors for endothelial vulnerability. These conditions constitute a biological substrate potentially favorable to gas bubble nucleation and stabilization, which are central mechanisms in the development of decompression sickness.**

Overall, these data support the hypothesis that hepatic steatosis, even in the absence of advanced liver damage, is capable of inducing a measurable pro-inflammatory cellular profile, strengthening the rationale for extending the study to in vivo models and for the comparative analysis of post-dive responses in subjects with and without NAFLD.

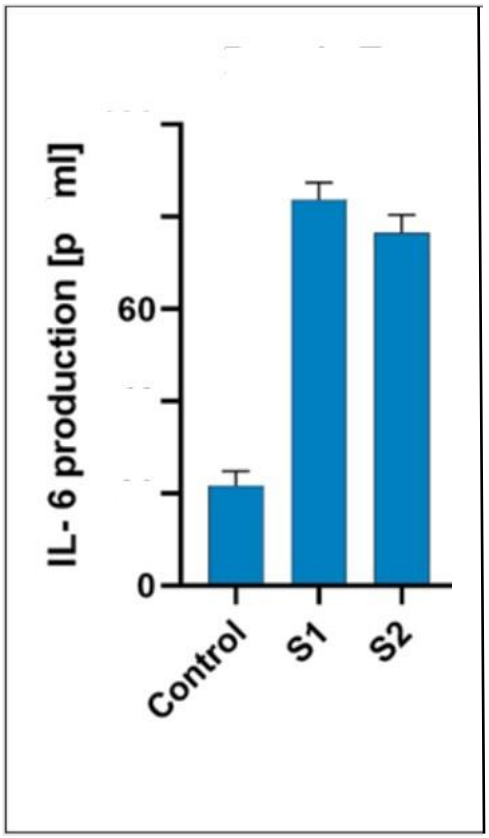

Figure 6.1 – *Production of the pro-inflammatory cytokine IL-6 in control HepG2 cells and in cells with induced NAFLD.* Source: original graph drawn based on assessments conducted on cell samples cultured at the laboratories of the University of Urbino Carlo Bo – Enrico Mattei Campus (2022–2025).

6.1.3 Inflammatory patterns and molecular mediators in steatotic cells: potential links with DCS

One of the central aspects in the study of NAFLD concerns chronic low-grade inflammatory response, characterized by a progressive increase in the production of pro-inflammatory cytokines and oxidative stress mediators. These patterns, also observable in steatotic HepG2 models, represent a fundamental component in the progression from steatosis to NASH (non-alcoholic steatohepatitis) and may potentially contribute to systemic endothelial dysfunction, reduced gas clearance, and altered mitochondrial response, all phenomena potentially involved in the genesis of DCS[73].

Among the main cytokines that show a significant increase in the scientific literature in steatotic HepG2 models are:

- **TNF-α (Tumor Necrosis Factor α)** – a central regulator of systemic inflammation, capable of inhibiting insulin signaling and inducing hepatocellular apoptosis;
- **IL-6 (Interleukin 6)** – mediator of the acute response and activation of the JAK/STAT pathway, with effects on coagulation and increased thrombotic risk;
- **IL-8 (Interleukin 8)** – a powerful neutrophil chemoattractant associated with oxidative stress and fibrotic processes;
- **MCP-1 (Monocyte Chemoattractant Protein-1)** – a key element in the activation of the hepatic inflammatory cascade and fibrogenesis.

These are accompanied by markers of oxidative stress such as MDA (malondialdehyde) and 4-HNE (4-hydroxy-2-nonenal), as well as a significant reduction in antioxidant enzymes (SOD, CAT, GPx), which testify to an impairment of the endogenous antioxidant response[74].

This redox imbalance not only amplifies cellular damage but also predisposes to phenomena of endothelial and pro-coagulant activation, elements already described as biological triggers in gas bubble formation in decompression sickness.

Recent evidence further indicates that a similar pro-inflammatory microenvironment may favor the formation and expansion of **Active Hydrophobic Spots (AHS)** on the endothelial surface, i.e., micro-

[73] Farrell, G. C., & van Rooyen, D. (2012). *NASH as an Inflammatory Disorder: Implications for Oxidative Stress and Endothelial Dysfunction.* Gut Liver, 6(2), 149–171.
[74] Parmar, S. R., et al. (2023). *Oxidative Stress-Mediated Liver Injury in Steatosis.* Frontiers in Pharmacology, 14, 1122457.

areas with gas-nucleating properties[75]. According to the model proposed by Arieli and subsequently confirmed by observations by Imbert and collaborators, these spots would represent a plausible pathophysiological substrate underlying "undeserved" DCS, thus providing a theoretical bridge between hepatic steatosis and decompression vulnerability[76]-[77] (as already described previously in this thesis 1.6.3).

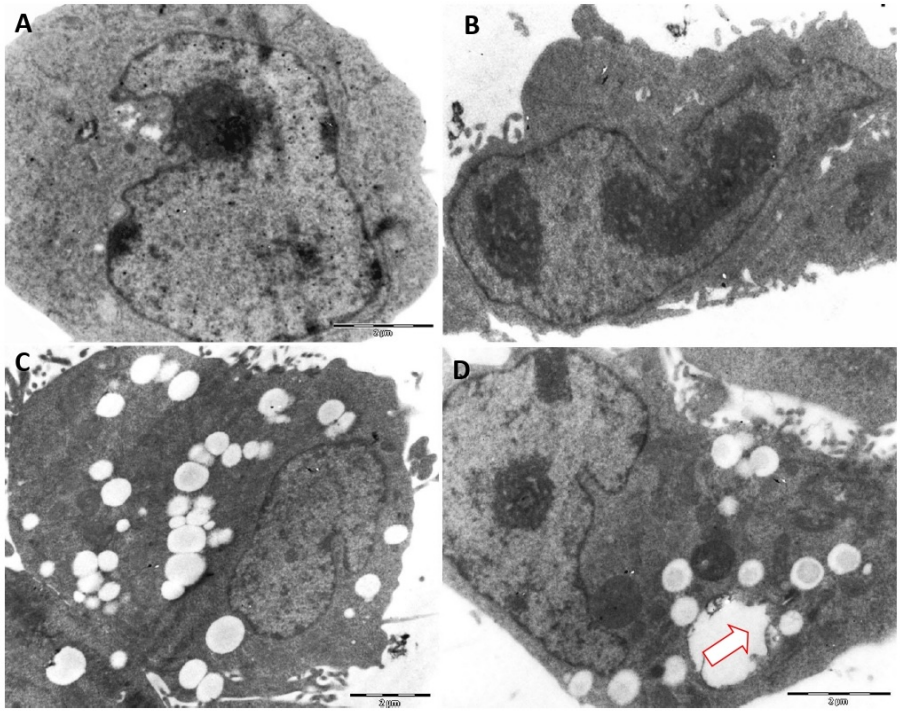

Figure 6.2 – *A–B: Control HepG2 cells. C–D: HepG2 cells treated with palmitic acid and oleic acid. In treated samples C and D, the intracellular accumulation of clear lipid-containing vesicles is evident; these occupy part of the cellular volume and leave impressions on larger organelles, such as the nucleus in C. Arrow = mitochondrial degeneration.* Source: original images acquired in the laboratory at the University of Urbino Carlo Bo – Enrico Mattei Campus (2023)

[75] Arieli, R. (2017). *Nanobubbles and Active Hydrophobic Spots as Contributors to Decompression Illness.* Journal of Applied Physiology, 122(2), 385–392.
[76] Imbert, J. P., Cialoni, D., Sponsiello, N., et al. (2019). *Static Metabolic Bubbles as Precursors of Vascular Gas Emboli.* Frontiers in Physiology, 10, 1453.
[77] Arieli, R. (2019a). *Decompression Bubbles: Pathophysiology and Clinical Relevance.* Diving and Hyperbaric Medicine, 49(3), 137–144.

6. 2 In vivo experimental study in recreational divers: design and methodology

The in vivo component of the present doctoral project was conceived to systematically explore the interactions between non-alcoholic fatty liver disease (NAFLD) and the formation of asymptomatic post-dive gas microbubbles, a phenomenon recognized as a potential risk marker for decompression sickness (DCS) [78] events, assessed through cardiac and vascular ultrasound (subclavian and jugular) performed thirty minutes after the conclusion of the experimental dry dive in a hyperbaric chamber. The pathophysiological hypothesis underlying this experimental approach stems from the observation - still insufficiently investigated in the literature - that chronic inflammatory conditions and metabolic alterations such as those associated with NAFLD may modify the endothelial response to hyperbaric exposure, increasing vascular vulnerability and facilitating gas nucleation during the ascent phase[79].

In other words, the presence of low-grade hepato-metabolic dysfunction, characterized by systemic inflammation, oxidative stress, and altered endothelial homeostasis, could represent a biological predisposing factor for the formation of Vascular Gas Emboli (VGE) even in the absence of decompression errors. This scenario justifies the need for a direct experimental investigation that integrates post-dive echocardiographic and vascular assessments with individual hepatic and metabolic parameters.

6.2.1 Dry hyperbaric chamber dive design and sample selection

The in vivo study was conducted at the **"Domus Medica" Center for Underwater and Hyperbaric Medicine of the Republic of San Marino**, in collaboration with the **University of Urbino "Carlo Bo" – Enrico Mattei Scientific Campus**, following favorable approval from the University Ethics Committee of Urbino (2023).

Thirty regularly active recreational divers were recruited, all holding a valid certification for dives up to 30 meters or deeper and having performed at least one dive in the previous six months. Participants' age ranged from 18 to 65 years, with a mean age of 41 ± 9 years and a male-to-female ratio of 22/8.

---

[78] Vann R. D., Butler F. K., Mitchell S. J., Moon R. E. (2011). *Decompression Illness. Lancet*, 377(9760), 153–164.
[79] Arieli R. (2019a). *Decompression Bubbles: Pathophysiology and Clinical Relevance. Diving and Hyperbaric Medicine*, 49(3), 137–144.

The inclusion criteria for the study comprised:

- absence of known major cardiovascular, respiratory, or metabolic comorbidities;
- no previous history of decompression sickness (DCS) during their diving career;
- absence of equalization difficulties at the time of the experiment, assessed by otoscopic examination;
- absence of clinical signs of acute inflammation of the upper airways or active sinusitis, which would have contraindicated the hyperbaric chamber test;
- possession of regular general medical fitness for diving according to current guidelines;
- signature of informed consent and consent for data processing (GDPR).

Based on these inclusion (and exclusion) criteria, all subjects summoned for the preliminary visit were enrolled in the hyperbaric chamber experiment, as no medical or technical contraindications to participation emerged[80].

This preparatory phase ensured **sample homogeneity**, minimization of bias related to external factors, and full safety of participants during the hyperbaric tests.

6.2.2 Pre-dive clinical and hepatic ultrasound assessment

In a first phase, each participant underwent a standardized clinical evaluation, including:

- **a complete medical history**, with particular attention to medical history, dietary habits, alcohol consumption, physical activity, and smoking;
- **a general physical examination** and recording of main vital parameters (arterial blood pressure, heart rate, arterial O_2 saturation), as well as cardiac and thoracic auscultation and otoscopy;
- **review of recent blood tests**, focusing on liver markers (AST, ALT, γGT, bilirubin), lipid profile, glycemia, and complete blood count.

[80] Doolette D. J. (2016). *Venous Gas Emboli and Decompression Sickness: The Link and the Limits. Undersea & Hyperbaric Medicine*, 43(5), 541–549.

All data were entered into a database created using Microsoft Excel. Subsequently, following the above assessment, each subject underwent abdominal liver ultrasound, performed by an experienced sonographer, with the aim of identifying the presence and degree of hepatic steatosis according to the standard ultrasound classification (mild, moderate, or severe steatosis)[81]. This evaluation was conducted in a blinded manner, so that divers were not informed of the result before the hyperbaric chamber session, thus avoiding possible psychological or behavioral conditioning related to the information.

6.2.3 Simulated "dry" dive in hyperbaric chamber

The experiment was carried out at "Domus Medica," Center for Hyperbaric Medicine of the Republic of San Marino, by means of a simulated dry dive in a hyperbaric chamber, conducted in a controlled clinical environment and monitored by a multidisciplinary team of underwater, hyperbaric, and resuscitation physicians.

The adopted dive profile was as follows:

- equivalent depth: 30 meters (4 ATA);
- bottom time: 25 minutes;
- controlled ascent according to the standard decompression protocol for recreational dives (U.S. Navy Table guidelines);
- breathing of ambient air (FiO_2 = 21%), without the use of oxygen-enriched mixtures, exactly the same type of air present in scuba cylinders.

The use of a dry model made it possible to eliminate environmental variables typical of real diving (temperature, movement, muscular effort), ensuring the same dive profile for all participants[82].

[81] Riazi K., Azhari H., Charette J. H., et al. (2022). *The Prevalence and Incidence of NAFLD Worldwide: A Systematic Review and Meta-Analysis. Lancet Gastroenterol Hepatol.*, 7, 851–861.
[82] Cialoni D., Pieri M., Marroni A. (2017). *Hyperbaric Exposure and Subclinical Vascular Stress: Methodological Considerations. Eur J Appl Physiol.*, 117(11), 2129–2140.

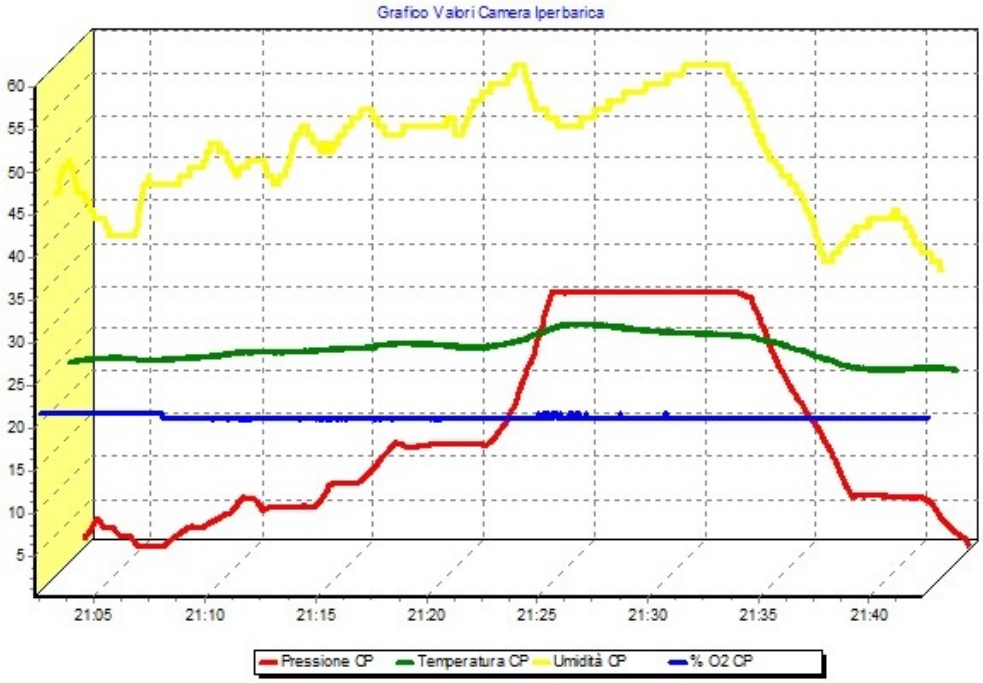

Figure 6.3 – *Graph showing the dry hyperbaric chamber dive profile used during the research project tests to simulate a standardized underwater dive at 30 meters.* Source: 'Domus Medica' Hyperbaric Medicine Center – Republic of San Marino (2024)

6.2.4 Post-dive cardiac and vascular ultrasound assessment for bubble detection

Thirty minutes after the end of the hyperbaric chamber dive, each participant underwent transthoracic echocardiography (apical "four-chamber" view) and vascular ultrasound of the jugular and subclavian vessels, performed at the Center for Underwater and Hyperbaric Medicine of San Marino by a cardiologist experienced in cardiac and vascular ultrasound. The primary objective was to detect gas bubbles in the venous circulation, considered an index of **subclinical decompression**.

Measurements were carried out in two consecutive phases:

1. at rest, for the baseline assessment of microbubble presence;
2. after the Valsalva maneuver, useful to temporarily increase intrathoracic pressure and promote bubble formation.

Results were coded according to the modified Spencer scale, which allows a semi-quantitative classification of bubble density and distribution in the right heart.

The comparison between subjects with and without NAFLD was organized for multivariate statistical analysis in collaboration with the **Department of Statistics of the University of Urbino**.

6. 3 Ultrasound detection of venous gas emboli (VGE): pathophysiological rationale and methodological validity

The use of transthoracic cardiac and vascular ultrasound for the detection of *venous gas emboli* (VGE) after scuba diving is currently a well-established and scientifically justified method in diving medicine, even in the absence of clinical manifestations of decompression sickness (DCS), as it allows the identification of "bubble-prone" individuals who are therefore at higher risk of DCS. This technique, initially introduced for experimental monitoring purposes in the 1980s, has evolved to become a standardized tool for assessing "decompression stress," owing to its non-invasiveness, repeatability, and capacity for objective quantification of the embolic phenomenon[83].

From a pathophysiological standpoint, the presence of VGE reflects the release of inert gas (mainly nitrogen) from tissues during ascent and represents its subclinical manifestation. The amount, distribution, and persistence of bubbles are considered indirect indicators of tissue saturation and of the organism's ability to eliminate dissolved gases[84]. Therefore, ultrasound makes it possible to transform a phenomenon that until a few years ago was largely theoretical - microbubble formation - into a measurable and comparable physiological parameter.

[83] Nishi R. Y., Kisman K. E., et al. (1988). *Assessment of Decompression Stress by Precordial Doppler Ultrasound Monitoring. Undersea Biomedical Research*, 15(1), 27–38.
[84] Papadopoulou V., Eckersley R. J., Balestra C., et al. (2018). *Circulatory Bubble Dynamics: From Physical to Biological Aspects. Advances in Colloid and Interface Science*, 256, 239–249.

6. 4 Scientific foundations and methodological rationale for ultrasound use

Ultrasound detection of bubbles provides a quantitative measure of "decompression stress," that is, the organism's response to pressure changes.

Even in **asymptomatic** divers, the appearance of VGE indicates that a transition of gas to the gaseous phase has occurred, constituting a useful marker for assessing the safety of decompression profiles[85]-[86].

6. 5 Individual variability in bubble production

Numerous studies have documented marked interindividual heterogeneity in VGE formation, even under identical depth, bottom time, and temperature conditions. Some individuals - defined as "bubble-prone" - tend to produce a high number of bubbles without exhibiting clinical symptoms, suggesting the existence of genetic, metabolic, or endothelial factors that modulate individual susceptibility[87]-[88] and that make it possible - as in this experiment - to investigate the patterns and physical characteristics that may explain bubble formation under otherwise comparable conditions.

6. 6 Correlation between bubble density and DCS risk

Although **the presence of VGE does not necessarily imply the onset of DCS**, an increase in the density and persistence of bubbles in the venous circulation is associated with a **higher relative risk of clinical decompression events**. Therefore, the ultrasound quantification of bubbles according to

[85] Doolette D. J. (2016). *Venous Gas Emboli and Decompression Sickness: The Link and the Limits. Undersea & Hyperbaric Medicine*, 43(5), 541–549.
[86] Karimpour M., Barak M., Arieli R. (2022). *Ultrasound Detection of Vascular Gas Emboli After Diving: Current Insights and Clinical Applications. Frontiers in Physiology*, 13, 863221.
[87] Hess H. W., et al. (2021). *Individual Variability in Bubble Formation After Standardized Dives. European Journal of Applied Physiology*, 121(10), 2863–2872.
[88] Imbert J. P., Egi S. M., Germonpré P., Balestra C. (2019). *Static Metabolic Bubbles as Precursors of Vascular Gas Emboli During Divers' Decompression. Frontiers in Physiology*, 10, 807.

the modified Spencer scale is currently considered a validated surrogate for assessing decompression risk in divers[89]-[90].

6. 7 Safety, reproducibility, and applicability in operational settings

Transthoracic echocardiography, vascular ultrasound, and Doppler are non-invasive methods, free from biological risks and easily repeatable, even in operational or field research contexts.

This makes them ideal tools for prospective studies or serial monitoring[91].

6. 8 Purpose of post-dive cardiac and vascular ultrasound

Finally, the ultrasound assessment of VGE can support an approach of "personalized decompression," identifying subjects with a high bubble-prone response and adapting decompression profiles accordingly. This paradigm falls within the broader vision of predictive and preventive diving medicine, which integrates physiological, metabolic, and vascular data in risk management[92]-[93].

The use of post-dive ultrasound in the present research project made it possible to objectively correlate the post-dive vascular response with the presence of NAFLD, providing new interpretative tools to understand how chronic metabolic conditions may influence individual vulnerability to "undeserved" DCS.

---

[89] Spencer M. P. (1976). *Decompression Limits for No-Dives and Their Relation to Venous Gas Emboli Detected by Doppler Ultrasonography. Undersea Biomedical Research*, 3(3), 253–260.
[90] Eftedal O., Brubakk A. O. (1997). *Detection of Intravascular Gas Bubbles Using Ultrasound: A Review.Ultrasound in Medicine & Biology*, 23(6), 901–918.
[91] Valić Z., et al. (2005). *Use of Echocardiography and Doppler for Non-Invasive Detection of Vascular Gas Emboli in Divers. Clinical Physiology and Functional Imaging*, 25(6), 348–352.
[92] Balestra C., Germonpré P., Marroni A. (2021). *Towards a Personalized Decompression Approach: The Role of Physiology and Preconditioning. Frontiers in Physiology*, 12, 727324.
[93] Arieli R. (2017). *Nanobubbles and Active Hydrophobic Spots as Contributors to Decompression Illness. Frontiers in Physiology*, 8, 591.

6. 9 Pathophysiological rationale: NAFLD, chronic inflammation, and endothelial vulnerability

The decision to compare the post-dive response between divers with and without hepatic steatosis is based on a growing body of evidence describing NAFLD as a multisystem condition capable of profoundly influencing endothelial and vascular metabolism[94]. NAFLD is typically associated with three key alterations:

- increased production of pro-inflammatory cytokines (TNF-α, **IL-6**, IL-1β), with amplification of the systemic inflammatory response;
- activation of hepatic and vascular oxidative stress, with reduced bioavailability of nitric oxide (NO) and loss of normal vasodilatory function;
- endothelial dysfunction, characterized by increased leukocyte adhesion, altered permeability, and a pro-coagulant state[95].

These changes generate a vulnerable endothelial substrate, predisposed to the formation and persistence of microbubbles during decompression, also in accordance with the model of Active Hydrophobic Spots (AHS) [96].

The integration of the results obtained from this in vivo phase with the in vitro data will provide a hypothetical pathophysiological basis for understanding the molecular mechanisms of individual susceptibility, potentially contributing to the definition of predictive biomarkers useful in the preventive assessment of decompression risk.

[94] Greco D., Kotronen A., Westerbacka J., et al. (2008). *Gene Expression in Human NAFLD. Am J Physiol Gastrointest Liver Physiol.*, 294, G1281–G1287.
[95] Bechmann L. P., Gieseler R. K., et al. (2010). *Apoptosis and CD36/Fatty Acid Translocase Upregulation in Non-Alcoholic Steatohepatitis. Liver Int.*, 30, 850–859.
[96] Imbert J. P., Cialoni D., Sponsiello N., et al. (2019). *Static Metabolic Bubbles as Precursors of Vascular Gas Emboli. Frontiers in Physiology*, 10, 1453.

Chapter 7 – Statistical analysis

7. 1 Materials and methods – Study design and participants

A cross-sectional observational study was conducted on a cohort of 30 certified divers (age 27–71 years; mean ± SD = 52.47 ± 12.05 years). The aim of the investigation was to assess, by means of abdominal ultrasound with hepatic focus, the presence of non-alcoholic fatty liver disease (NAFLD) and subsequently to explore the relationship between cardiovascular and metabolic variables and the formation of cardiac microbubbles detected by echocardiography and vascular ultrasound after a dry dive in a hyperbaric chamber, following a standardized profile (as described in Chapter 6).

Participants were recruited among active divers with varying levels of activity, quantified as the average number of dives per year (0–10; 10–20; >20). All subjects completed a structured clinical lifestyle questionnaire; prior to data collection, the main anthropometric parameters (weight, height, and BMI) were measured, with a mean BMI ± SD of 26.74 ± 3.71 kg/m², and participants underwent a medical examination.

7.1.1 Variables

The dependent variable of the study was the semi-quantitative echocardiographic bubble index (ecoCARDIO), ranging from 0 to 3, used to describe the extent of post-dive cardiac microbubble formation (Figure 6.1 and Figure 6.2).

Independent variables included continuous predictors such as:

- Age (years) – (Figure 6.3)
- BMI (kg/m²) – (Figure 6.4 and Figure 6.5)

and categorical predictors related to lifestyle and clinical conditions:

- Ultrasound diagnosis of non-alcoholic fatty liver disease (NAFLD) (yes/no)
- Average annual number of dives 0–10 (Figure 6.7)
- Average annual number of dives 10–20 (Figure 6.8)
- Average annual number of dives > 20 (Figure 6.9)

- Smoking – yes/no (Figure 6.10)
- Arterial hypertension – yes/no (Figure 6.11)
- Cardiovascular disease – yes/no (Figure 6.12)
- Metabolic disease – yes/no (Figure 6.13)
- Family history of cardiovascular/metabolic disorders – yes/no (Figure 6.14)
- Impaired fasting glucose (GLYCEMIA) – yes/no (Figure 6.15)
- Altered lipid profile (Assetto_LIP) – yes/no (Figure 6.16)
- Altered hepatic profile (Assetto_EPAT) – yes/no (Figure 6.17)
- Use of cardiovascular drugs – yes/no (Figure 6.18)
- Use of antidiabetic drugs – yes/no (Figure 6.19)
- Use of lipid-lowering drugs – yes/no (Figure 6.20)
- Use of drugs for joint diseases – yes/no (Figure 6.21)
- Use of drugs for gastrointestinal disorders – yes/no (Figure 6.22)
- Use of drugs for urological conditions – yes/no (Figure 6.23)

7.1.2 Statistical analysis

For all quantitative variables, descriptive statistics were calculated (mean, standard deviation, range), whereas for qualitative variables frequencies and percentages were reported.

For multivariate analysis, an ANCOVA (Analysis of Covariance) was performed using a backward stepwise elimination procedure, with ecoCARDIO as the dependent variable. Predictors were iteratively removed based on goodness-of-fit criteria (Akaike Information Criterion, AIC; Mallows' Cp) until identifying the model with the best compromise between parsimony and explanatory power. Multicollinearity was assessed using the Variance Inflation Factor (VIF) and Tolerance; VIF values below 3.4 were considered indicative of acceptable collinearity. The overall quality of the model was described using R^2, adjusted R^2, MSE, and RMSE; independence of residuals was examined using the Durbin–Watson statistic. **A two-tailed p-value < 0.05 was considered statistically significant.**

7. 2 Results

7.2.1 Descriptive statistics

The mean number of post-dive cardiac microbubbles detected (ecoCARDIO) was 0.98 ± 1.13 (range 0–3). The mean age of the divers was 52.47 years, with an overall anthropometric profile consistent with moderate overweight (mean BMI 26.74 kg/m²).

Regarding diving exposure, the majority of participants reported fewer than 10 dives per year (76.7%); 23.3% reported 10–20 dives per year, while a relevant proportion declared more than 20 dives annually. Comorbidities and risk factors were relatively infrequent: arterial hypertension and smoking were each present in 26.7% of subjects, whereas cardiovascular and metabolic diseases were reported in 10% of participants. From a therapeutic standpoint, 13.3% were taking lipid-lowering medications and 10% were receiving treatment for diabetes management.

7.2.2 Descriptive comparison of bubble count in relation to NAFLD presence

The distribution of ecoCARDIO was represented using a box-and-whisker plot in order to compare values between subjects with and without ultrasound diagnosis of NAFLD (Figure 6.1).

The descriptive analysis shows that, in the NAFLD group, **there is a tendency toward higher central values (median and mean) of microbubble count compared to the group without steatosis**. Moreover, in the NAFLD group a greater dispersion of values is observable, consistent with a wider interindividual variability of the post-dive bubble phenomenon; **conversely, in the group without NAFLD the distribution appears more concentrated, with overall lower values**.

Although this is an exploratory and descriptive representation, **the overall trend suggests that the presence of NAFLD may be associated with a greater propensity to form cardiac and vascular microbubbles after controlled diving**. Since all dives were conducted under standardized conditions (identical exposure profile in terms of depth and duration), the observed differences are plausibly largely attributable to individual characteristics of the subjects, in line with the hypothesis of increased “bubble-proneness” in the presence of hepatic/metabolic alterations.

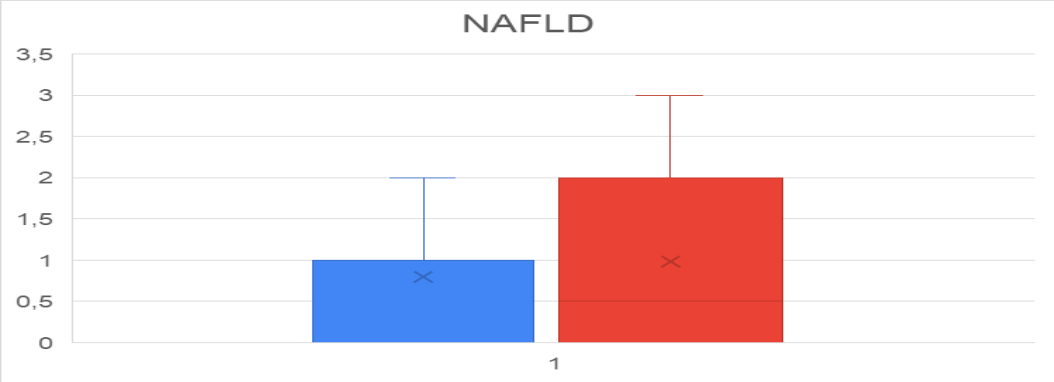

Figure 7.1– *Comparison of the number of ultrasound-detected bubbles in relation to the presence of NAFLD. The graph shows the distribution of the number of bubbles detected at echocardiographic examination (y-axis) in subjects without NAFLD (absence, left) and with NAFLD (presence, right), allowing a comparison between the two groups.*
Source: statistical data processing by Prof. Davide Sisti, Department of Biomolecular Sciences (DISB), University of Urbino Carlo Bo (2025)

7.2.3 Correlations and multicollinearity

The Pearson correlation matrix showed a moderate positive association between age and ecoCARDIO ($r = 0.53$), whereas BMI displayed a weak correlation ($r = 0.07$), suggesting a limited contribution of the latter to the variability of the bubble index in the analyzed sample.

Among categorical variables, altered hepatic profile (Assetto_EPAT) and the use of cardiovascular or lipid-lowering medications were among those most strongly associated with bubble formation. The collinearity assessment revealed Tolerance values > 0.34 and VIF < 3.4, supporting the absence of problematic multicollinearity among the predictors included in the final model.

7.2.4 ANCOVA model selection

The backward elimination procedure was initiated with 16 predictors, leading to a final model consisting of four variables:

- Age;
- Assetto_EPAT (altered hepatic profile);
- Use of cardiovascular drugs;
- Use of lipid-lowering drugs.

The final model represented the best compromise between simplicity and predictive accuracy according to the adopted criteria (AIC = –3.83; Cp = –1.78; PC = 0.72).

7.2.5 Model quality

The goodness of fit of the model was moderate, with $R^2 = 0.485$ and adjusted $R^2 = 0.403$. The mean squared error was MSE = 0.757 (RMSE = 0.870), and the Durbin–Watson statistic of 1.69 suggested overall acceptable independence of residuals.

7.2.6 Analysis of variance

The overall ANCOVA was statistically significant (Table 6.1), indicating that the set of selected predictors explains a significant proportion of the variability in echocardiographic microbubble formation.

Table 7.1 – *Results of the analysis of covariance (ANCOVA) on the number of echocardiographic microbubbles.* Source: statistical data processing by Prof. Davide Sisti, Department of Biomolecular Sciences (DISB), University of Urbino Carlo Bo (2025).

Source	df	SS	MS	F	p-value
Model	4	17.82	4.46	5.89	0.0018
Error	25	18.92	0.76		
Corrected total	29	36.74			

The table reports the decomposition of the total variance in terms of model, error, and corrected total, with the corresponding degrees of freedom (df), sums of squares (SS), mean squares (MS), F statistic, and p-value. The overall ANCOVA is statistically significant (p = 0.0018), indicating that the set of selected predictors explains a significant proportion of the variability in echocardiographic microbubble formation.

7.2.7 Model parameters

The model coefficients (Table 6.2) indicate a positive trend of age with respect to the ecoCARDIO index (B = +0.0298; p = 0.067), close to statistical significance. The use of cardiovascular drugs (B = –0.930; p = 0.041) was associated with a reduction in ecoCARDIO, whereas the use of lipid-

lowering drugs also showed an association oriented toward a reduction of the index, with a result at the borderline of significance (B = –1.020; p = 0.053). The variable altered Assetto_EPAT showed a negative coefficient (B = –1.447; p = 0.120), without reaching statistical significance in the analyzed sample.

Table 7.2 – Coefficients of the regression model (ANCOVA) for the number of echocardiographically detected microbubbles (ecoCARDIO). Source: statistical data processing by Prof. Davide Sisti, Department of Biomolecular Sciences (DISB), University of Urbino Carlo Bo (2025)

Predictor	Coeff. (B)	SE	t	p	IC 95%	β
Intercept	2.415	1.552	1.56	0.132	–0.78 ; 5.61	—
Age (years)	+0.0298	0.0156	1.91	0.067	–0.002 ; 0.062	0.319
Altered Assetto_EPAT	–1.447	0.899	–1.61	0.120	–3.30 ; 0.41	–0.235
Cardiovascular drugs	–0.930	0.431	–2.16	0.041	–1.82 ; –0.04	–0.355
Lipid-lowering drugs	–1.020	0.503	–2.03	0.053	–2.06 ; 0.02	–0.313

For each predictor included in the model, the table reports the unstandardized coefficient (B), the standard error (SE), the t statistic, the p-value, the 95% confidence interval (95% CI), and the standardized coefficient (β). The results highlight a statistically significant negative association for the use of cardiovascular drugs (p = 0.041) and associations close to statistical significance for age and for the use of lipid-lowering drugs.

7.2.8 Estimated marginal means

The estimated marginal means highlight differences between the levels of the categorical variables included in the model. For Assetto_EPAT, the non-altered profile showed an estimated mean of 1.56 ± 0.27 (95% CI: 0.99–2.12), whereas the altered profile displayed a mean of 3.00 ± 0.94 (95% CI: 1.07–4.94).

Regarding cardiovascular drugs, the absence of therapy was associated with an estimated mean of 1.82 ± 0.49 (95% CI: 0.80–2.83), while the presence of therapy corresponded to 2.75 ± 0.63 (95% CI: 1.44–4.05).

Similarly, for lipid-lowering drugs, “no” corresponded to 1.77 ± 0.48 (95% CI: 0.79–2.76) and “yes” to 2.79 ± 0.67 (95% CI: 1.41–4.17).

7. 3 Interpretation of the results

Overall, the ANCOVA model suggests that age tends to increase the degree of post-dive bubble formation, with a result close to statistical significance ($p = 0.067$). This trend is consistent with known phenomena in vascular pathophysiology, including the progressive reduction in endothelial elasticity, increased arterial stiffness, and microcirculatory changes associated with aging, which may be relevant to gas exchange and transport dynamics.

In parallel, the observed association for the use of cardiovascular and lipid-lowering drugs, oriented toward a lower microbubble burden (significant for cardiovascular drugs and borderline for lipid-lowering drugs), suggests a possible modulatory effect on vascular and microcirculatory determinants involved in bubble-proneness. Although causality cannot be inferred in a cross-sectional observational design, this pattern is compatible with the hypothesis that better control of cardiovascular and metabolic risk may influence functional parameters of the endothelium and tissue perfusion, impacting conditions that facilitate bubble nucleation and persistence.

The altered hepatic profile (Assetto_EPAT), although not reaching statistical significance ($p = 0.120$), is in continuity with the descriptive evidence from the NAFLD yes/no comparison and with the biological rationale of the project. In this context, NAFLD and, more broadly, alterations in hepatic profile can be interpreted as markers of an underlying metabolic-inflammatory state potentially associated with endothelial vulnerability and greater interindividual variability in post-dive response.

Overall, the model explains approximately 48.5% of the total variance in the ecoCARDIO index, outlining a combined contribution of age and variables related to cardiovascular and metabolic health on post-dive microcirculatory outcomes. The pathophysiological discussion and integration with in vitro experimental results will be developed in the following chapters (Chapters 8 and 9), with particular attention to the role of inflammatory mediators and markers of endothelial dysfunction as possible determinants of individual susceptibility to decompression sickness.

7. 4 Figures and graphs

Table 7.3 – Descriptive statistics of the analyzed quantitative variables. Source: statistical data processing by Prof. Davide Sisti, Department of Biomolecular Sciences (DISB), University of Urbino Carlo Bo (2025)

Descriptive statistics (Quantitative data):						
Statistics	NAFLD eco 2 (FIXED ULTRASOUND)	ecoCARDIO (bubbles)	Age	Weight (kg)	Height (cm)	BMI
No. Of obstervations	30	30	30	30	30	30
Minimum	0,000	0,000	27,000	54,000	167,000	19,362
Maximum	2,000	3,000	71,000	114,000	184,000	37,654
1st quartile	0,000	0,000	44,000	74,000	170,000	24,454
Median	1,000	0,500	55,000	80,500	175,500	26,028
3rd quartile	1,000	2,000	62,000	89,500	178,750	28,407
Mean	0,800	0,983	52,467	81,667	174,667	26,738
Variance (n-1)	0,579	1,267	145,223	147,471	21,954	13,766
Standard deviation (n-1)	0,761	1,126	12,051	12,144	4,686	3,710

The table reports the main descriptive statistics (number of observations, minimum and maximum values, quartiles, median, mean, variance, and standard deviation) for the ultrasound variables (NAFLD eco 2, ecoCARDIO), anthropometric variables (age, weight, height), and body mass index (BMI) of the study sample (n = 30).

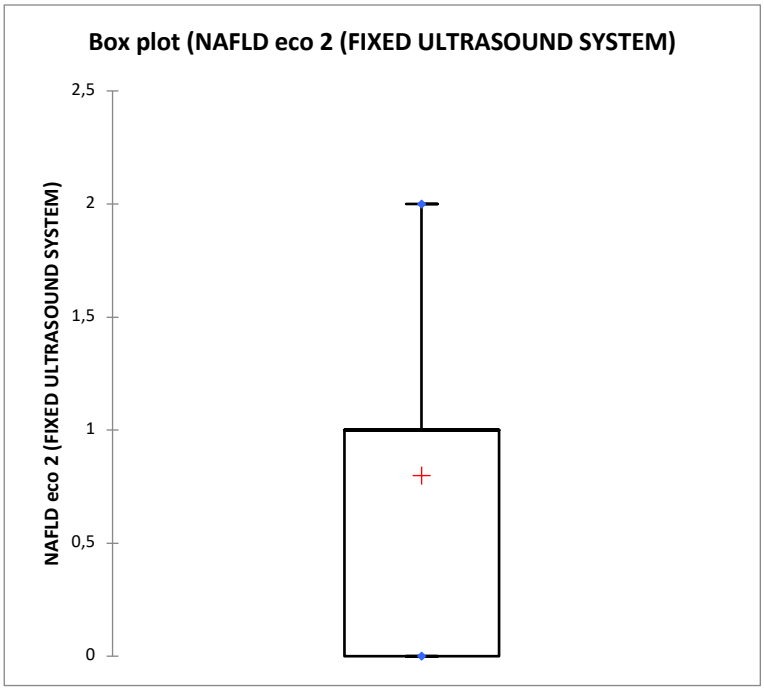

Figure 7.2 – *Box plot of the distribution of NAFLD eco2 values detected using a fixed ultrasound system. The box plot represents the distribution of NAFLD eco2 values, highlighting the minimum value, the first and third quartiles, the median, and the possible presence of outliers.*
Source: statistical data processing by Prof. Davide Sisti, Department of Biomolecular Sciences (DISB), University of Urbino Carlo Bo (2025)

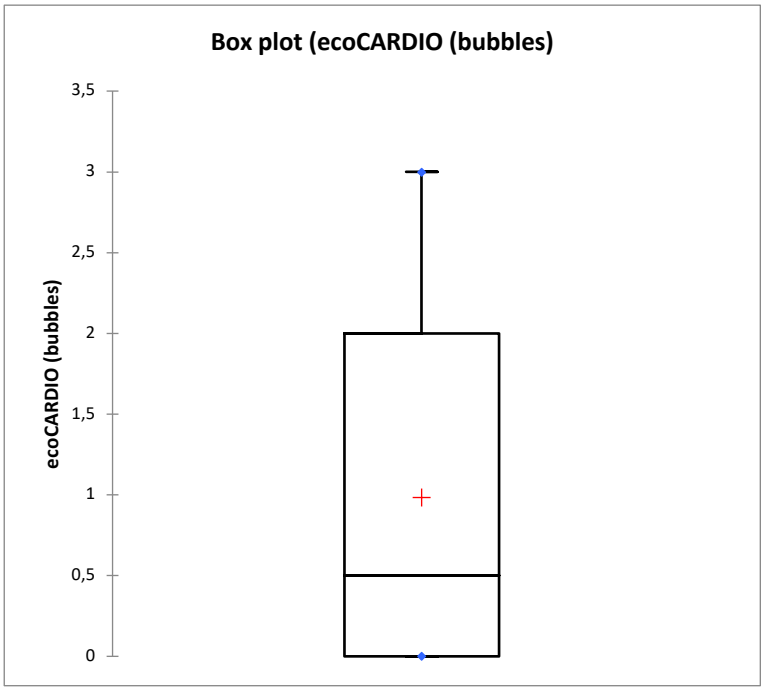

Figure 7.3 – *Box plot of the distribution of ecoCARDIO (bubble) values. The box plot represents the distribution of ecoCARDIO values, highlighting the minimum value, the first and third quartiles, the median, and the range of observed values, allowing an assessment of the variability of the measurement in the analyzed sample.*
Source: statistical data processing by Prof. Davide Sisti, Department of Biomolecular Sciences (DISB), University of Urbino Carlo Bo (2025)

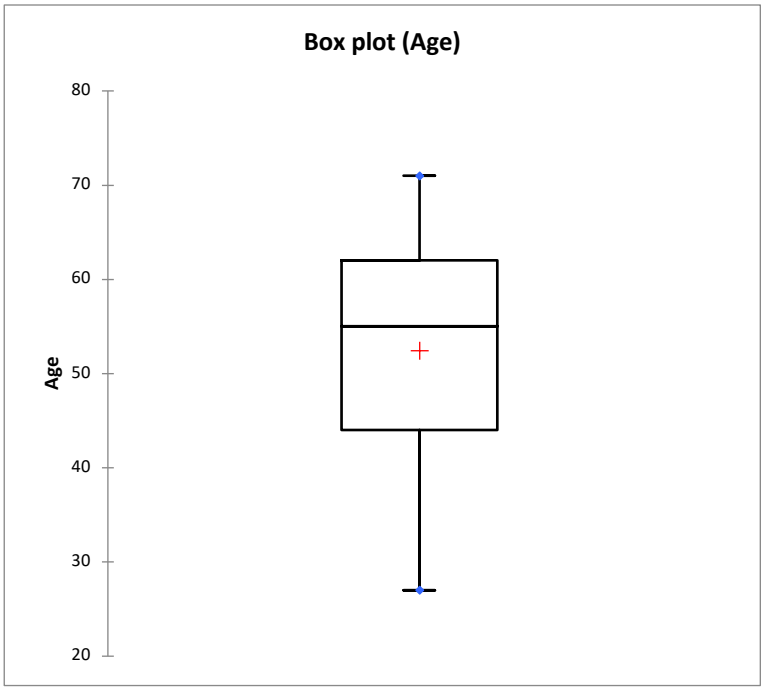

Figure 7.4 – *Box plot of the age distribution of the study sample. The box plot represents the distribution of age values, highlighting the minimum value, the first and third quartiles, the median, and the range of observed values, allowing an assessment of the demographic variability of the analyzed sample.*
Source: statistical data processing by Prof. Davide Sisti, Department of Biomolecular Sciences (DISB), University of Urbino Carlo Bo (2025)

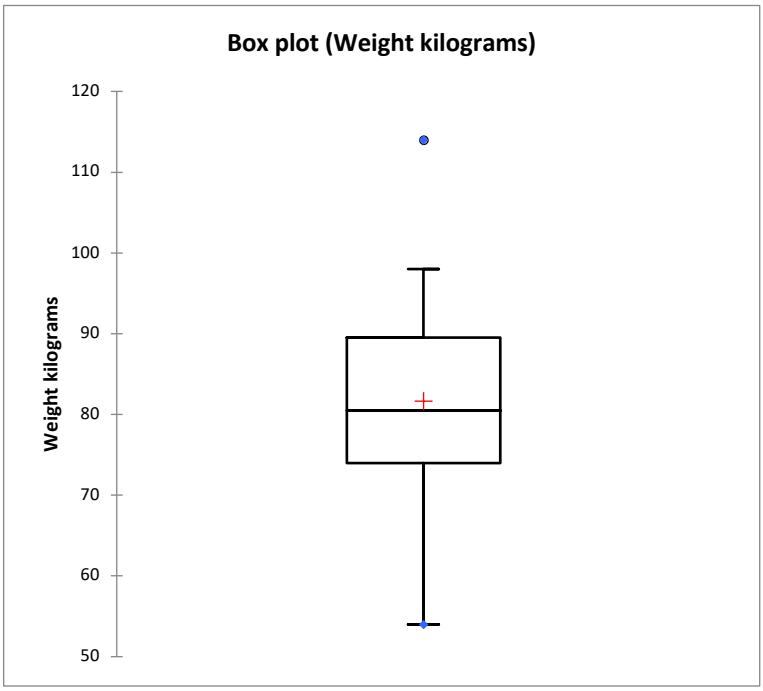

Figure 7.5 – *Box plot of the distribution of body weight (kg) of the study sample. The box plot represents the distribution of body weight values, highlighting the minimum value, the first and third quartiles, the median, and the range of observed values, allowing an assessment of the weight variability of the analyzed sample.*
Source: statistical data processing by Prof. Davide Sisti, Department of Biomolecular Sciences (DISB), University of Urbino Carlo Bo (2025)

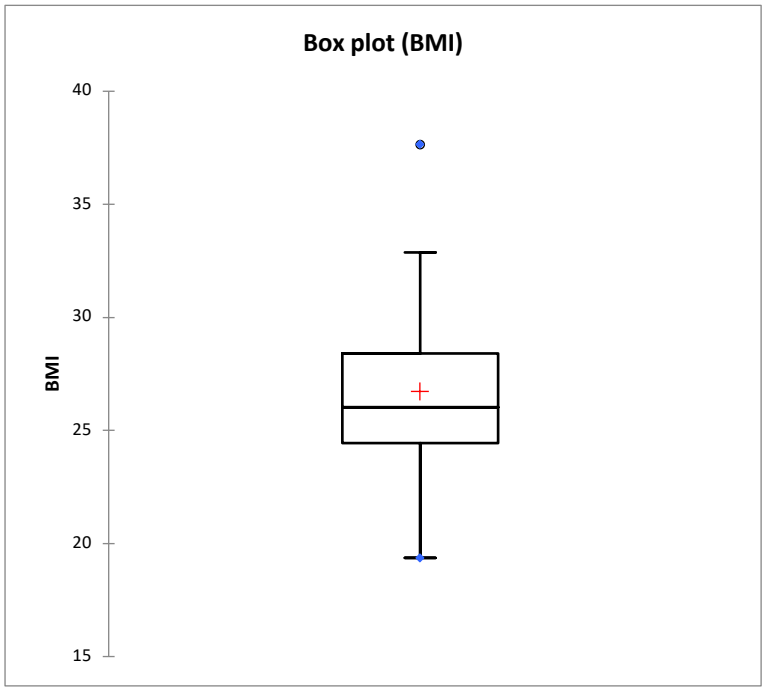

Figure 7.6– *Box plot of the distribution of body mass index (BMI) of the study sample. The box plot represents the distribution of BMI values, highlighting the minimum value, the first and third quartiles, the median, and the range of observed values, allowing an assessment of the variability of weight status in the analyzed sample.*
Source: statistical data processing by Prof. Davide Sisti, Department of Biomolecular Sciences (DISB), University of Urbino Carlo Bo (2025)

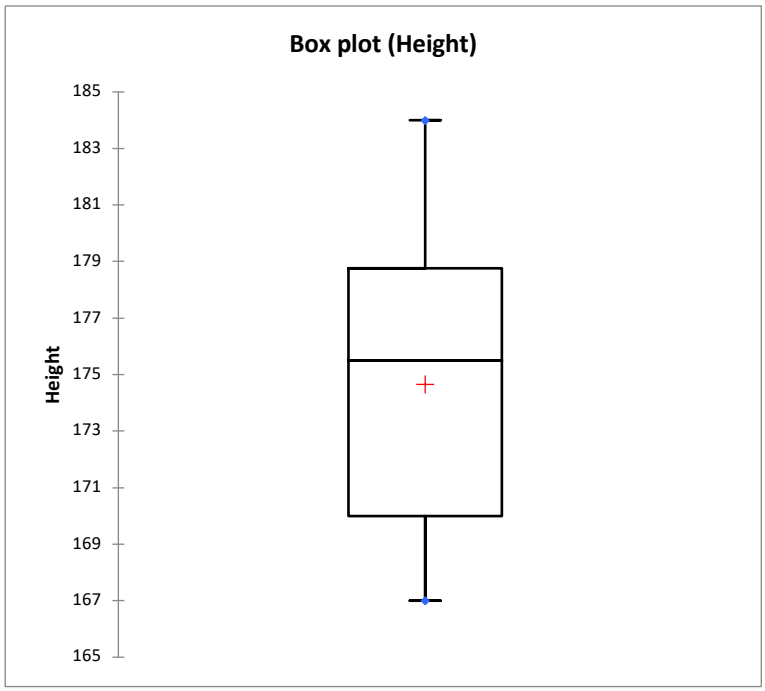

Figure 7.7 – *Box plot of the distribution of height (cm) of the study sample. The box plot represents the distribution of height values, highlighting the minimum value, the first and third quartiles, the median, and the range of observed values, allowing an assessment of the stature variability of the analyzed sample.*
Source: statistical data processing by Prof. Davide Sisti, Department of Biomolecular Sciences (DISB), University of Urbino Carlo Bo (2025)

Table 7.4 – Descriptive statistics of the qualitative variables of the sample. Source: statistical data processing by Prof. Davide Sisti, Department of Biomolecular Sciences (DISB), University of Urbino Carlo Bo (2025).

Variable	Category	Frequency	Frequency %	95% CI freq. lower	95% CI freq. upper	Proportion	95% CI prop. lower	95% CI prop. upper
Average dives/year (0–10)	No (0)	23	76,667	61,532	91,802	0,767	0,615	0,918
	Yes (1)	7	23,333	8,198	38,468	0,233	0,082	0,385
Average dives/year (10–20)	No (0)	19	63,333	46,089	80,577	0,633	0,461	0,806
	Yes (1)	11	36,667	19,423	53,911	0,367	0,194	0,539
Average dives/year (>20)	No (0)	18	60,000	42,470	77,530	0,600	0,425	0,775
	Yes (1)	12	40,000	22,470	57,530	0,400	0,225	0,575
Smoking	No (0)	22	73,333	57,509	89,158	0,733	0,575	0,892
	Yes (1)	8	26,667	10,842	42,491	0,267	0,108	0,425
High blood pressure	No (0)	22	73,333	57,509	89,158	0,733	0,575	0,892
	Yes (1)	8	26,667	10,842	42,491	0,267	0,108	0,425
Cardiovascular diseases	No (0)	27	90,000	79,265	100,000	0,900	0,793	1,000
	Yes (1)	3	10,000	0,000	20,735	0,100	0,000	0,207
Metabolic diseases	No (0)	27	90,000	79,265	100,000	0,900	0,793	1,000
	Yes (1)	3	10,000	0,000	20,735	0,100	0,000	0,207
Family history of disease	No (0)	17	56,667	38,934	74,399	0,567	0,389	0,744
	Yes (1)	13	43,333	25,601	61,066	0,433	0,256	0,611
Blood glucose	No (0)	23	76,667	61,532	91,802	0,767	0,615	0,918
	Yes (1)	7	23,333	8,198	38,468	0,233	0,082	0,385
Lipid profile	No (0)	19	63,333	46,089	80,577	0,633	0,461	0,806
	Yes (1)	11	36,667	19,423	53,911	0,367	0,194	0,539
Liver function tests	No (0)	29	96,667	90,243	100,000	0,967	0,902	1,000
	Yes (1)	1	3,333	0,000	9,757	0,033	0,000	0,098
Cardiovascular medications	No (0)	23	76,667	61,532	91,802	0,767	0,615	0,918
	Yes (1)	7	23,333	8,198	38,468	0,233	0,082	0,385
Diabetes medications	No (0)	27	90,000	79,265	100,000	0,900	0,793	1,000
	Yes (1)	3	10,000	0,000	20,735	0,100	0,000	0,207
Lipid-lowering medications	No (0)	26	86,667	74,502	98,831	0,867	0,745	0,988
	Yes (1)	4	13,333	1,169	25,498	0,133	0,012	0,255
Joint disease medications	No (0)	29	96,667	90,243	100,000	0,967	0,902	1,000
	Yes (1)	1	3,333	0,000	9,757	0,033	0,000	0,098
Gastrointestinal medications	No (0)	29	96,667	90,243	100,000	0,967	0,902	1,000
	Yes (1)	1	3,333	0,000	9,757	0,033	0,000	0,098
Urological medications	No (0)	30	100,000	100,000	100,000	1,000	1,000	1,000

The table reports the distribution of absolute and relative frequencies of the qualitative variables analyzed, including response categories, modal frequency, percentages, 95% confidence intervals, and associated proportions. The variables considered relate to habits, clinical conditions, family history, and medication use in the study sample (n = 30)

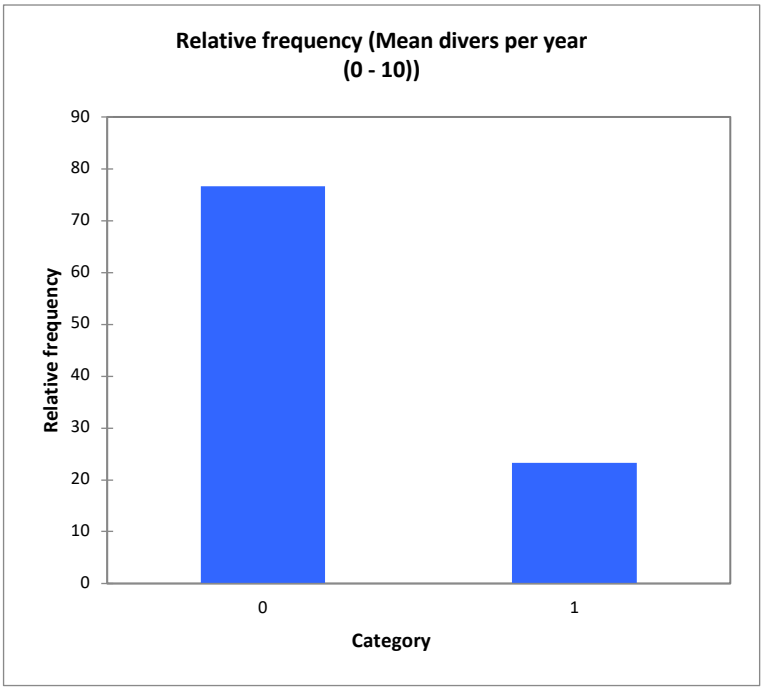

Figure 7.8 – *Relative frequency of subjects with an average annual number of dives between 0 and 10. Category 0 indicates the absence of dives in this range, while category 1 indicates the presence of dives in this range.*
Source: statistical data processing by Prof. Davide Sisti, Department of Biomolecular Sciences (DISB), University of Urbino Carlo Bo (2025)

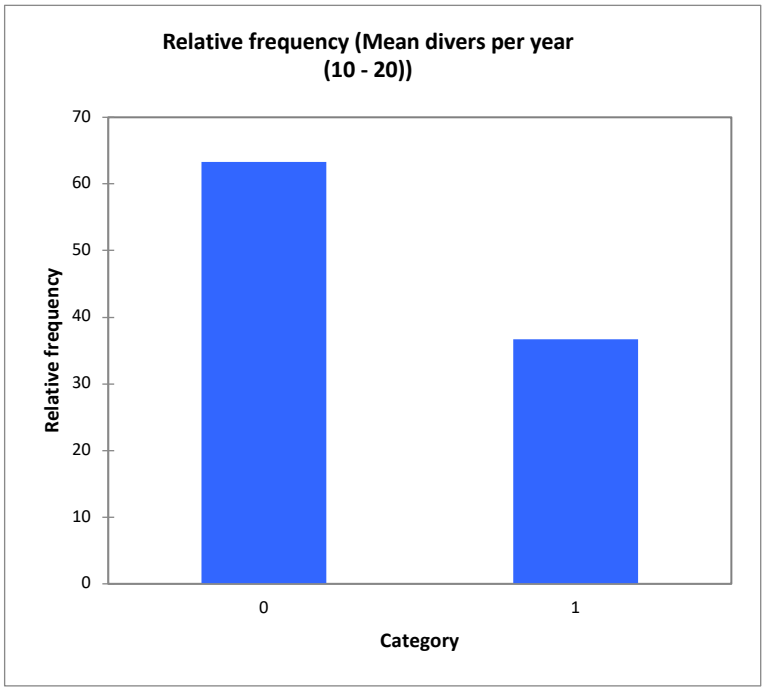

Figure 7.9 – *Relative frequency of subjects with an average annual number of dives between 10 and 20. Category 0 indicates subjects who do not belong to this range, while category 1 indicates subjects who belong to this range.*
Source: statistical data processing by Prof. Davide Sisti, Department of Biomolecular Sciences (DISB), University of Urbino Carlo Bo (2025)

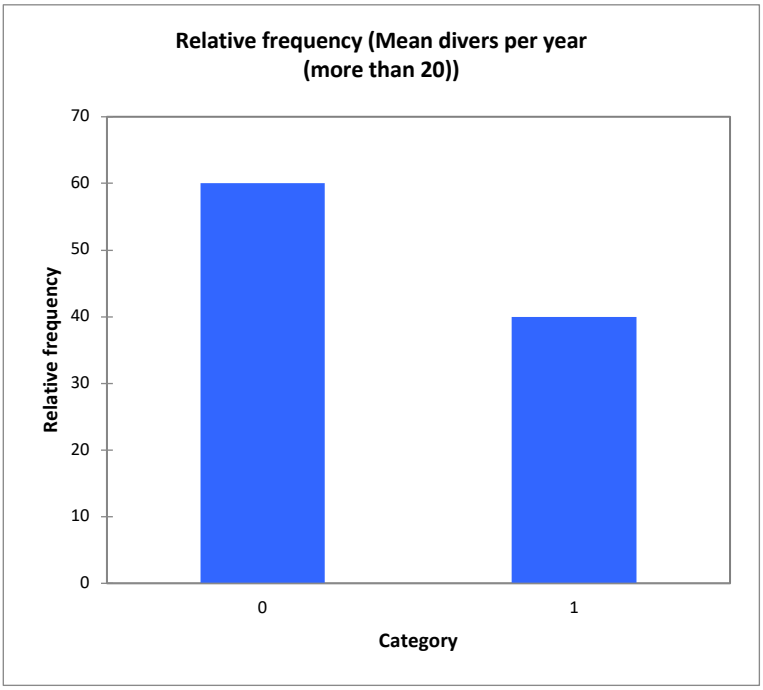

Figure 7.10 – *Relative frequency of subjects with an average annual number of dives greater than 20. Category 0 indicates subjects who do not belong to this range, while category 1 indicates subjects who belong to this range.*
Source: statistical data processing by Prof. Davide Sisti, Department of Biomolecular Sciences (DISB), University of Urbino Carlo Bo (2025)

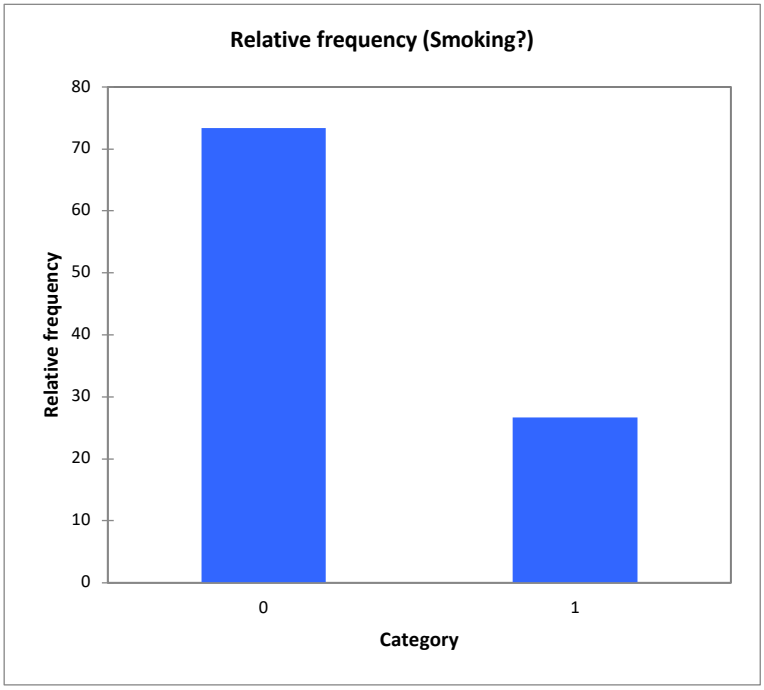

Figure 7.11 – *Relative frequency of subjects in relation to smoking habit. Category 0 indicates non-smokers, while category 1 indicates smokers.*
Source: statistical data processing by Prof. Davide Sisti, Department of Biomolecular Sciences (DISB), University of Urbino Carlo Bo (2025)

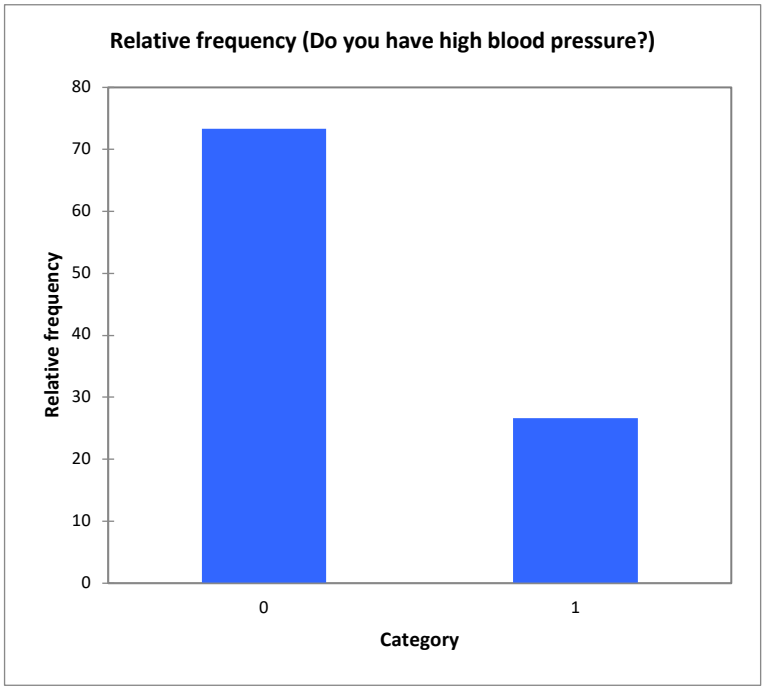

Figure 7.12 – *Relative frequency of subjects in relation to the presence of arterial hypertension. Category 0 indicates subjects who do not report arterial hypertension, while category 1 indicates subjects who report having it.*
Source: statistical data processing by Prof. Davide Sisti, Department of Biomolecular Sciences (DISB), University of Urbino Carlo Bo (2025)

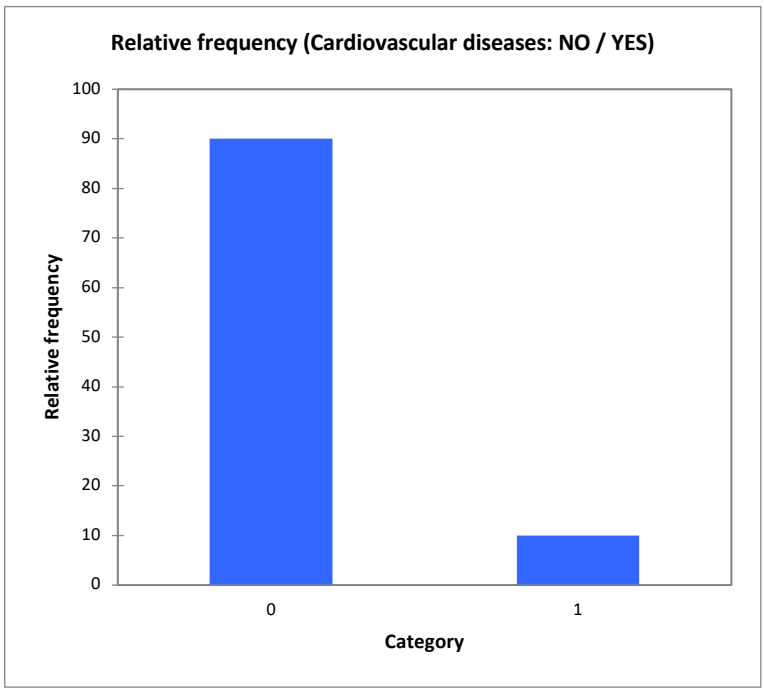

Figure 7.13 – *Relative frequency of subjects in relation to the presence of cardiovascular diseases. Category 0 indicates subjects who do not report the presence of cardiovascular diseases, while category 1 indicates subjects who report their presence.*
Source: statistical data processing by Prof. Davide Sisti, Department of Biomolecular Sciences (DISB), University of Urbino Carlo Bo (2025)

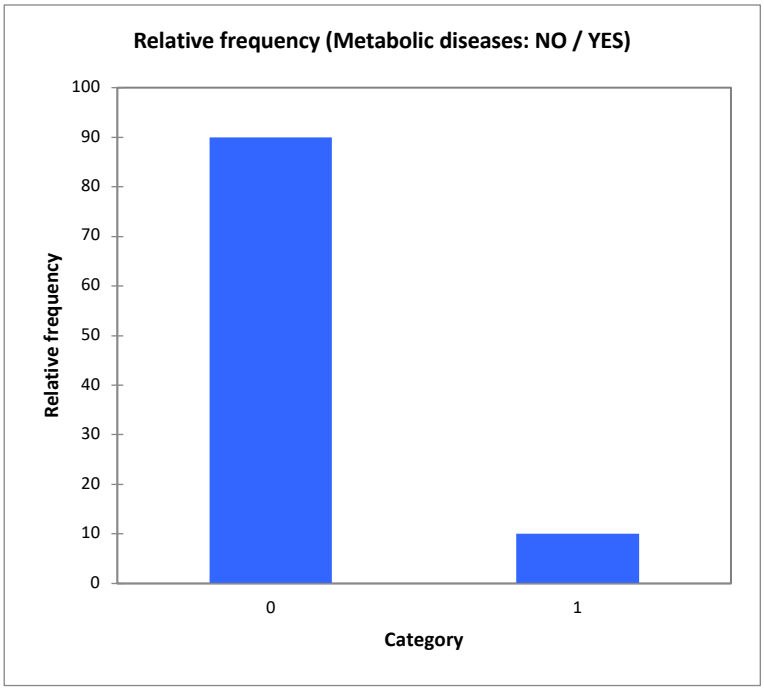

Figure 7.14 – *Relative frequency of subjects in relation to the presence of metabolic diseases. Category 0 indicates subjects who do not report the presence of metabolic diseases, while category 1 indicates subjects who report their presence.*
Source: statistical data processing by Prof. Davide Sisti, Department of Biomolecular Sciences (DISB), University of Urbino Carlo Bo

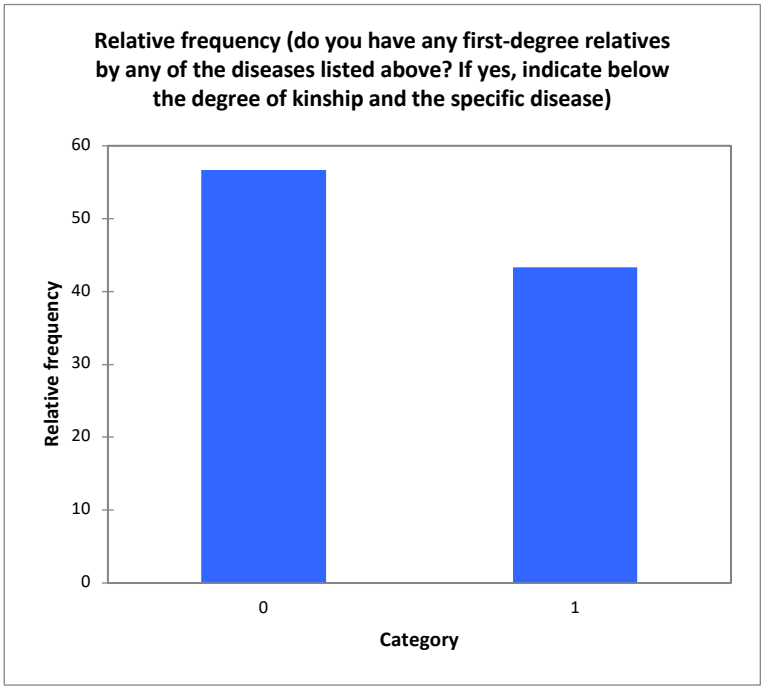

Figure 7.15 – *Relative frequency of subjects in relation to the presence of first-degree family history of the considered diseases. Category 0 indicates subjects who do not report a first-degree family history of the considered diseases, while category 1 indicates subjects who report the presence of at least one affected first-degree relative.*
Source: statistical data processing by Prof. Davide Sisti, Department of Biomolecular Sciences (DISB), University of Urbino Carlo Bo (2025)

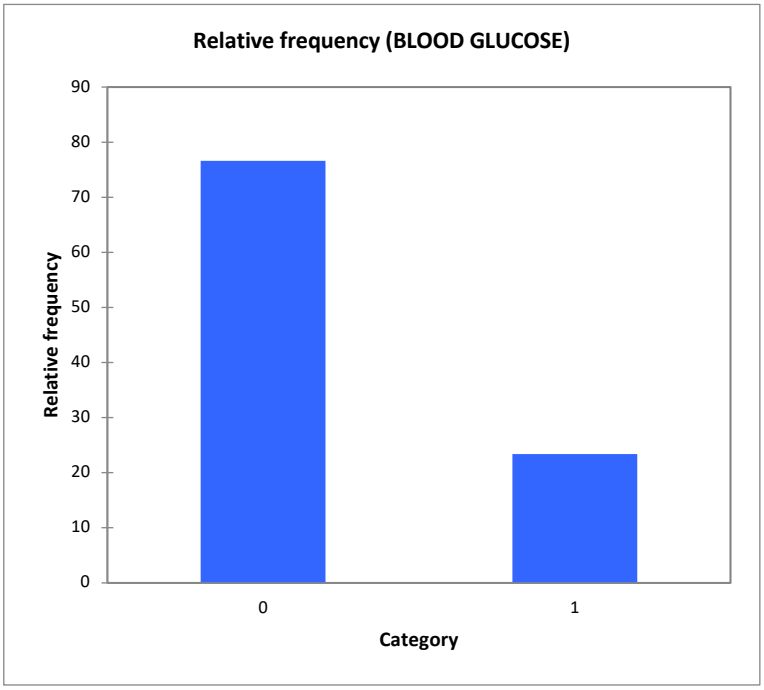

Figure 7.16 – *Relative frequency of subjects in relation to blood glucose levels. Category 0 indicates subjects who do not report altered glycemic values, while category 1 indicates subjects who report altered glycemic values.*
Source: statistical data processing by Prof. Davide Sisti, Department of Biomolecular Sciences (DISB), University of Urbino Carlo Bo (2025)

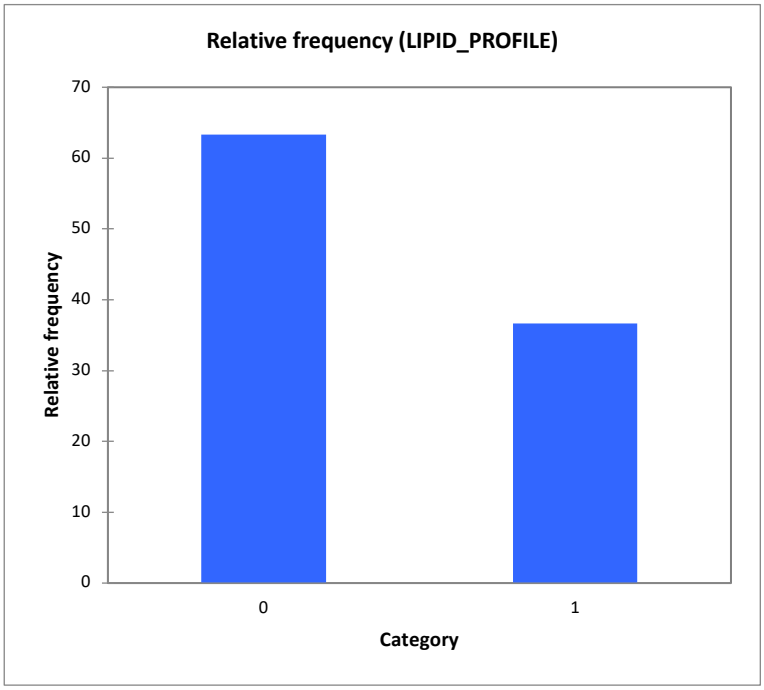

Figure 7.17– *Relative frequency of subjects in relation to lipid profile. Category 0 indicates subjects who do not report alterations in lipid profile, while category 1 indicates subjects who report alterations in lipid profile.*
Source: statistical data processing by Prof. Davide Sisti, Department of Biomolecular Sciences (DISB), University of Urbino Carlo Bo (2025)

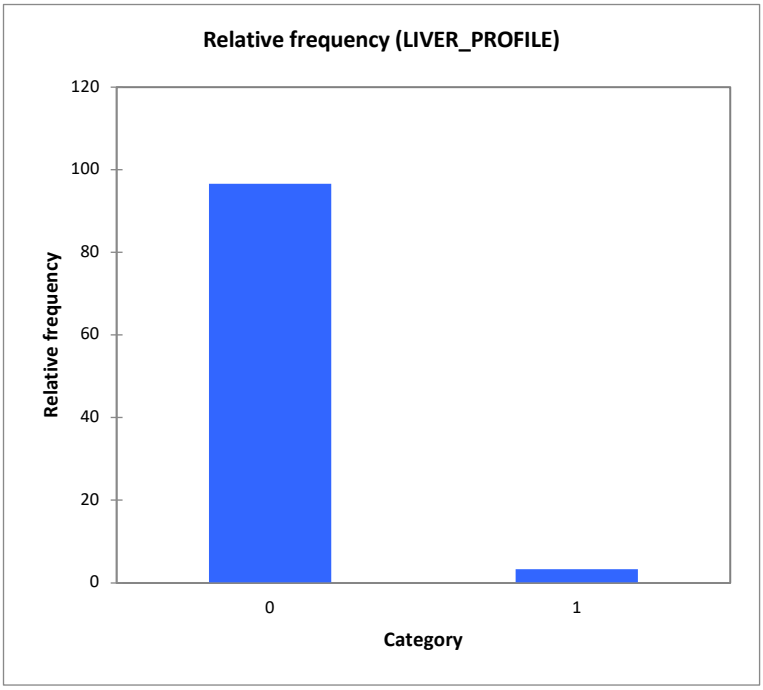

Figure 7.18 – *Relative frequency of subjects in relation to liver profile. Category 0 indicates subjects who do not report alterations in liver profile, while category 1 indicates subjects who report alterations in liver profile.*
Source: statistical data processing by Prof. Davide Sisti, Department of Biomolecular Sciences (DISB), University of Urbino Carlo Bo (2025)

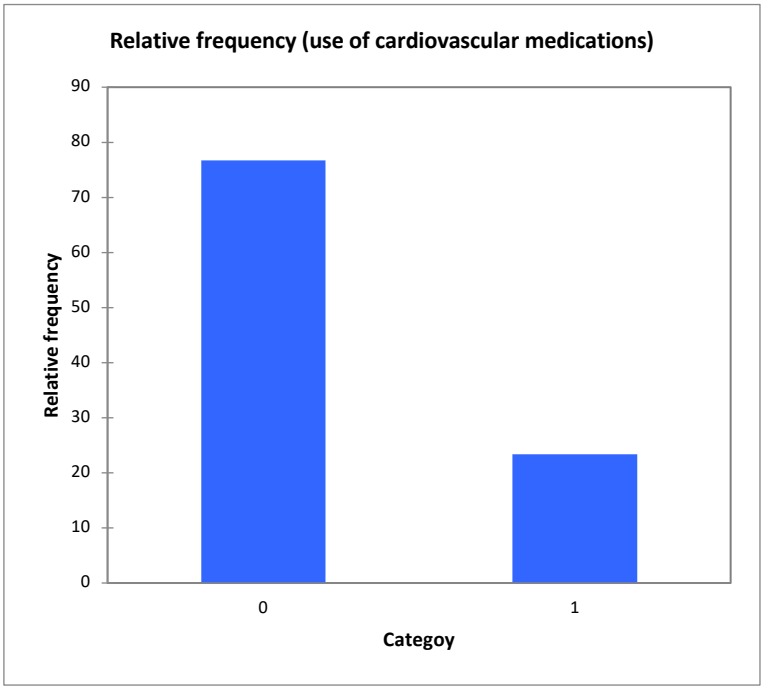

Figure 7.19 – *Relative frequency of subjects in relation to the use of medications for cardiovascular diseases. Category 0 indicates subjects who do not take medications for cardiovascular diseases, while category 1 indicates subjects who take medications for cardiovascular diseases.*
Source: statistical data processing by Prof. Davide Sisti, Department of Biomolecular Sciences (DISB), University of Urbino Carlo Bo (2025)

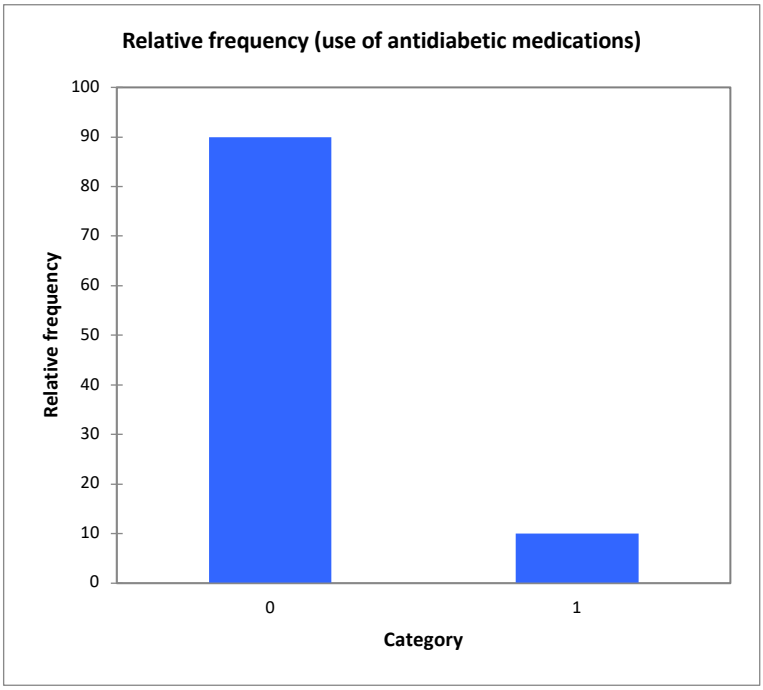

Figure 7.20 – *Relative frequency of subjects in relation to the use of medications for diabetes. Category 0 indicates subjects who do not take medications for diabetes, while category 1 indicates subjects who take medications for diabetes.*
Source: statistical data processing by Prof. Davide Sisti, Department of Biomolecular Sciences (DISB), University of Urbino Carlo Bo (2025)

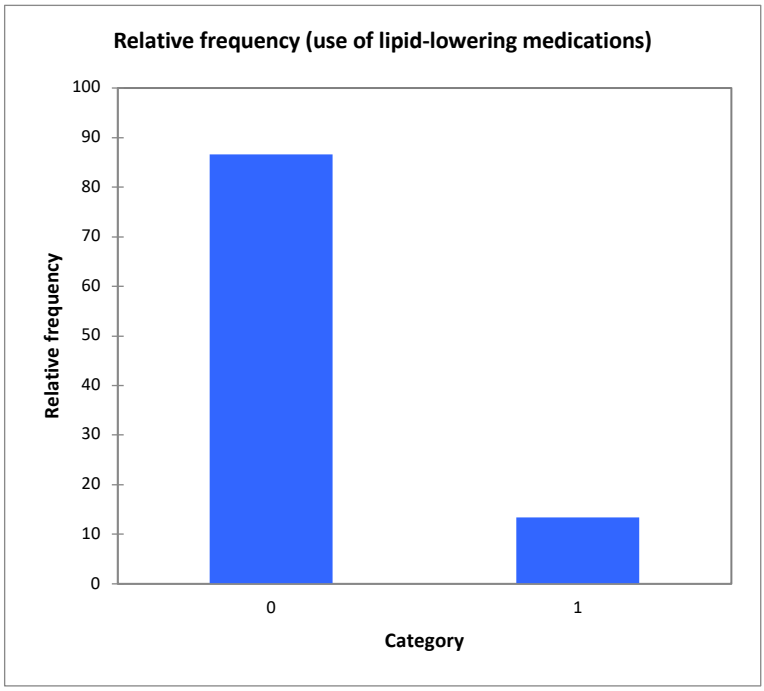

Figure 7.21 – *Relative frequency of subjects in relation to the use of medications for dyslipidemia. Category 0 indicates subjects who do not take medications for dyslipidemia, while category 1 indicates subjects who take medications for dyslipidemia.*
Source: statistical data processing by Prof. Davide Sisti, Department of Biomolecular Sciences (DISB), University of Urbino Carlo Bo (2025)

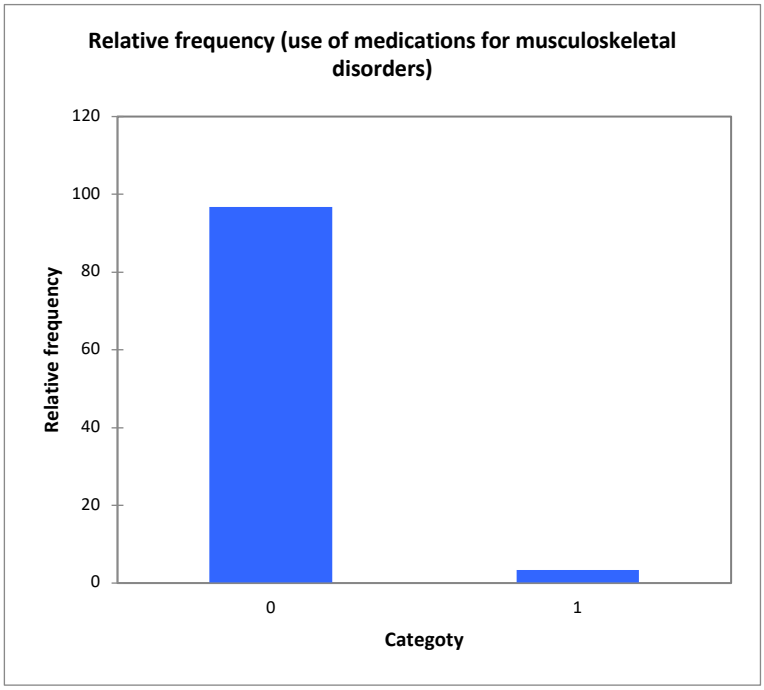

Figure 7.22 – *Relative frequency of subjects in relation to the use of medications for joint diseases. Category 0 indicates subjects who do not take medications for joint diseases, while category 1 indicates subjects who take medications for joint diseases.*
Source: statistical data processing by Prof. Davide Sisti, Department of Biomolecular Sciences (DISB), University of Urbino 'Carlo Bo' (2025)

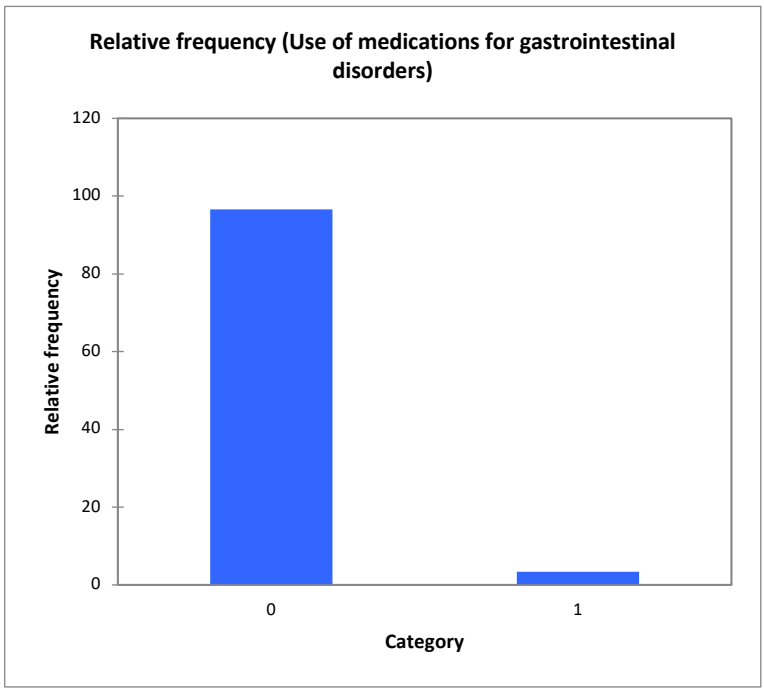

Figure 7.23 – *Relative frequency of subjects in relation to the use of medications for gastrointestinal diseases. Category 0 indicates subjects who do not take medications for gastrointestinal diseases, while category 1 indicates subjects who take medications for gastrointestinal diseases.*
Source: statistical data processing by Prof. Davide Sisti, Department of Biomolecular Sciences (DISB), University of Urbino 'Carlo Bo' (2025)

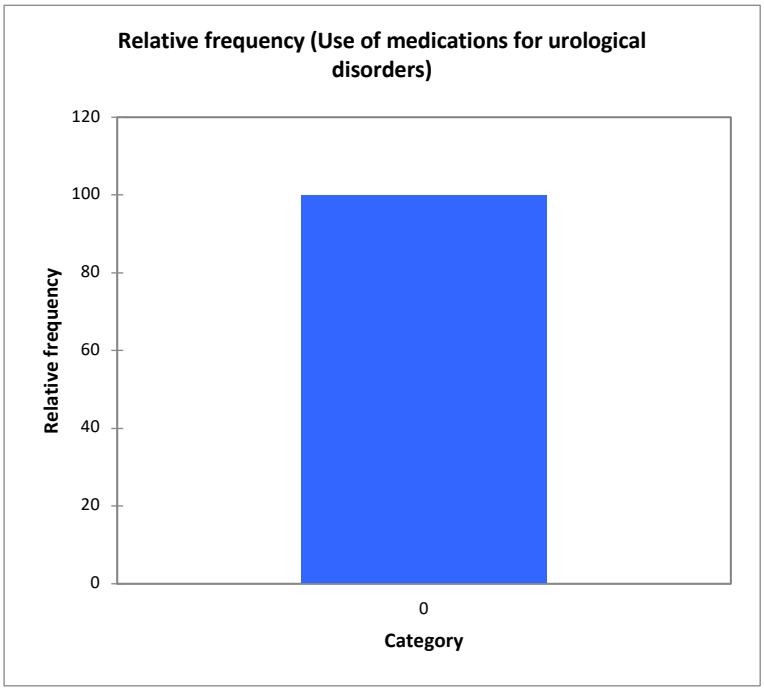

Figure 7.24 – *Relative frequency of subjects in relation to the use of medications for urological diseases. Category 0 indicates subjects who do not take medications for urological diseases, while category 1 indicates subjects who take medications for urological diseases.*
Source: statistical data processing by Prof. Davide Sisti, Department of Biomolecular Sciences (DISB), University of Urbino Carlo Bo (2025)

Chapter 8 – Discussion of the results

The present research project was conceived with the aim of systematically exploring the possible relationship between non-alcoholic fatty liver disease (NAFLD) and the formation of venous gas microbubbles (venous gas emboli, VGE) following a simulated dive in a hyperbaric chamber. VGE do not per se represent a direct indicator of decompression sickness (DCS), but are widely recognized in the literature as a marker of individual susceptibility to the decompression response. In this context, the study fits within the line of research aimed at understanding why, under the same hyperbaric exposure, some individuals develop a significantly higher bubble load than others, configuring a potential risk of so-called “undeserved” DCS.

8. 1 Pathophysiological framework and biological rationale

NAFLD is now considered a systemic disease, characterized by a state of chronic low-grade inflammation, alterations in lipid metabolism, and widespread endothelial dysfunction. Numerous lines of evidence indicate that these changes are not confined to the liver alone, but involve the microcirculation and vascular function at a systemic level. Based on this rationale, the hypothesis underlying the present work is that the presence of NAFLD may modulate the dynamics of microbubble formation during decompression, contributing to the definition of a profile of greater biological vulnerability.

It is important to emphasize that increased bubble production does not automatically equate to the development of clinical disease, but represents a sensitive indicator of the individual response to hyperbaric stress. From this perspective, the assessment of VGE assumes value not so much as a diagnostic tool, but rather as a pathophysiological and predictive one.

8. 2 Results of the in vivo study: individual variability and associated factors

The results of the study conducted on divers show that post-dive microbubble formation is a frequent phenomenon but characterized by marked interindividual variability. Since the hyperbaric exposure profile was rigorously standardized for all participants, this variability cannot be attributed to

differences in dive depth or duration, but most likely reflects intrinsic biological characteristics of the subjects.

In this context, age emerges as one of the main determinants of the decompression response. Older divers tend to exhibit a higher number of VGE compared to younger individuals, a finding consistent with the progressive decline in endothelial function, reduced vascular elasticity, and structural changes in the vessel wall associated with aging. This result aligns with the literature on vascular physiology and reinforces the notion that individual biology plays a central role in decompression dynamics.

A particularly interesting aspect concerns the **relationship between NAFLD and bubble formation**. The descriptive analysis and graphical representation show that subjects with hepatic steatosis tend to develop a higher number of VGE compared to those without NAFLD. Moreover, in the NAFLD group a wider dispersion of values is observed, indicating a more heterogeneous response, likely modulated by concomitant factors such as chronic inflammation, oxidative stress, and alterations in lipid metabolism.

These elements suggest that **hepatic steatosis may influence the decompression response**, although they do not allow the establishment of a direct causal relationship. The exploratory nature of the study and the limited sample size require a cautious interpretation of the results.

8. 3 Integration with the multivariate statistical model

The analysis using the ANCOVA model provides further interpretative elements. **In addition to age, altered hepatic profile and the use of cardiovascular and lipid-lowering drugs were associated with the number of bubbles**. In particular, the latter appear to correlate with a reduction in VGE load, suggesting a possible protective or modulatory effect on endothelial function.

It is plausible to hypothesize that better control of blood pressure and lipid profile contributes to stabilizing the vascular wall and reducing the predisposition to gas nucleation.

The result concerning NAFLD remains the most delicate to interpret. The observed trend, characterized by greater bubble-proneness in subjects with steatosis, is pathophysiologically plausible but does not reach **robust statistical significance**. This is likely related to the limited sample size and the observational nature of the study.

8. 4 Contribution of the in vitro study and biological coherence

The link with the in vitro experimental component nevertheless strengthens the biological coherence of the proposed model. Hepatic HepG2 cells subjected to steatotic induction show increased inflammatory activity, oxidative stress, and mitochondrial dysfunction, **with particular reference to the increased production of pro-inflammatory cytokines such as IL-6**. These conditions are known to promote endothelial dysfunction and alteration of cellular surfaces.

In light of the Active Hydrophobic Spots (AHS) model, **such changes could facilitate gas nucleation during the decompression phase, increasing the likelihood of microbubble formation**. Although the in vitro data and the in vivo findings do not demonstrate direct causality, the convergence between experimental evidence and clinical observations suggests the existence of a biologically plausible interaction between hepatic lipid metabolism and vascular pathophysiology.

8. 5 Role of IL-6 as a possible pathophysiological link between NAFLD and decompression sickness

The results obtained in the cellular model of induced hepatic steatosis show a significant and consistent increase in IL-6 production in steatotic HepG2 cells compared with controls, confirming the establishment of a pro-inflammatory microenvironment already at an early and experimentally controlled stage of intracellular lipid accumulation. This finding assumes particular relevance if interpreted not as an isolated hepatocellular phenomenon, but as a potential element of systemic connection between NAFLD and increased vulnerability to decompression sickness.

IL-6 is a pleiotropic cytokine, capable of acting both locally and systemically, with documented effects on endothelial function, vascular homeostasis, and regulation of coagulation mechanisms. In conditions of hepatic steatosis, increased IL-6 production by hepatocytes contributes to **a state of chronic low-grade inflammation**, which may be reflected systemically through activation of the vascular endothelium. Endothelium exposed to persistently elevated IL-6 levels shows altered vasomotor tone, increased expression of adhesion molecules, and greater permeability, configuring a state of subclinical endothelial dysfunction.

In the context of decompression sickness, **endothelial dysfunction represents a key element of modern pathophysiology**. It is known that the endothelium is not merely a passive target of gas bubbles, but an active player in modulating the inflammatory, thrombotic, and vascular response

induced by decompression. An endothelium already “primed” by a systemic inflammatory state, such as that potentially associated with NAFLD, may display a reduced capacity to adapt to the mechanical and biochemical stress induced by microbubble formation and gas passage across the endothelium, favoring their stabilization and amplifying their biological “bubble-forming” effects, which are central to the mechanisms underlying DCS.

In this scenario, IL-6 can be interpreted as a central mediator of vulnerability, capable of lowering the tolerance threshold of the endothelium to decompressive insults. The increased vascular permeability and activation of the coagulation cascade induced by IL-6 could facilitate the interaction between gas bubbles and the endothelium, promoting adhesion phenomena, platelet activation, and microthrombosis, described as early events in the clinical pathogenesis of “undeserved” decompression sickness.

Overall, the results of this study support the notion that the decompression response is strongly individual and biologically mediated. NAFLD may represent one of the factors capable of modulating this response, helping to explain some of the interindividual differences observed in microbubble formation and, potentially, certain cases of “undeserved” DCS.

However, at present, the evidence collected does not allow the conclusion that hepatic steatosis directly and independently increases the risk of decompression sickness. Rather, the data indicate the need for future studies on larger samples.

Chapter 9 – Conclusion

This research project has addressed in an integrated manner the possible relationship between non-alcoholic fatty liver disease (NAFLD) and the decompression response, combining an in vitro experimental approach with an in vivo observational study on divers undergoing simulated immersion in a hyperbaric chamber. The originality of this work lies in having explored a still poorly investigated area of diving medicine, proposing NAFLD not merely as a metabolic comorbidity, but as a potential biological determinant of individual susceptibility to the formation of venous gas emboli (VGE).

The in vitro experimental line demonstrated that the induction of steatosis in hepatic cells is associated with an increased inflammatory burden and cellular stress, particularly with respect to the production of pro-inflammatory cytokines such as IL-6. These findings support the hypothesis that hepatic steatosis configures a biological state characterized by mitochondrial dysfunction and chronic low-grade inflammation, conditions known to promote endothelial dysfunction and alter microvascular homeostasis. In this context, the cellular model provides a plausible mechanistic rationale through which hepatic alterations may influence vascular processes relevant to decompression physiology.

In parallel, the in vivo study showed that post-immersion microbubble formation is a common phenomenon but highly variable among individuals, even under a standardized hyperbaric exposure profile. Data analysis suggests that such variability is largely biologically mediated and influenced by individual clinical and metabolic factors. In particular, age, alterations in hepatic profile, and the use of cardiovascular and lipid-lowering medications emerge as relevant elements in modulating VGE burden. **Subjects with NAFLD show a tendency toward greater bubble formation, although this association does not reach full statistical significance, likely due to the intrinsic limitations of the sample size and observational design**.

Overall, the results do not allow the conclusion that NAFLD represents a certain and independent risk factor for “undeserved” decompression sickness. However, they consistently indicate that hepatic and metabolic health constitute a non-negligible component of the individual decompression response. From this perspective, NAFLD can be interpreted as a potential marker of biological vulnerability, capable of interacting with other vascular and microcirculatory determinants in defining susceptibility to microbubble formation.

This work therefore suggests a paradigm shift in diving risk assessment, moving beyond solely hyperbaric exposure parameters toward a broader vision that includes the subject's metabolic and inflammatory status. In the future, the assessment of metabolic, cardiovascular, and functional hepatic profile, as well as liver ultrasound screening for NAFLD, could become part of more personalized risk stratification strategies, aligned with the principles of precision medicine and the development of individualized decompression models.

Finally, this study represents an exploratory contribution that paves the way for further research on larger populations and with more advanced diagnostic methodologies. The integration of inflammatory and endothelial biomarkers, quantitative liver imaging techniques, and predictive statistical models may allow a more definitive clarification of the role of NAFLD in decompression pathophysiology and, more broadly, improve the safety of diving activities.

Declaration on the Use of Artificial Intelligence Tools (AI Usage Disclosure)

Some revisions of the manuscript were carried out with the support of generative artificial intelligence tools, used exclusively for editorial purposes, stylistic harmonization, and improvement of clarity of exposition. The vast majority of the drafting of the text, the argumentative structure, as well as the entire body of data, analyses, interpretations, results, conclusions, and scientific reasoning are the work of the Author, who guarantees their accuracy, methodological coherence, and full scientific responsibility.

BIBLIOGRAPHY

Arieli, R. (2017). Nanobolle e siti idrofobici attivi come contributori alla malattia da decompressione. *Frontiers in Physiology, 8*, 591.

Arieli, R. (2019a). Bolle da decompressione: fisiopatologia e rilevanza clinica. *Diving and Hyperbaric Medicine, 49*(3), 137–144.

Arieli, R. (2017). Meccanismi fisico-chimici della formazione di bolle nell'attività subacquea. *Journal of Applied Physiology, 122*(2), 385–392.

Arya, A., Patel, N., Mistry, S., et al. (2023). Disfunzione endoteliale e sindrome metabolica: implicazioni per la formazione di emboli gassosi vascolari. *Journal of Applied Physiology, 135*(1), 12–24.

Balestra, C., Germonpré, P., & Marroni, A. (2021). Verso un approccio personalizzato alla decompressione: ruolo della fisiologia e del precondizionamento. *Frontiers in Physiology, 12*, 727324.

Ballestri, S., et al. (2017). La NAFLD come malattia multisistemica: evidenze dalla pratica clinica. *Hepatology, 65*(4), 1137–1154.

Bechmann, L. P., Gieseler, R. K., et al. (2010). Apoptosi e sovraregolazione di CD36/Fatty Acid Translocase nella steatoepatite non alcolica. *Liver International, 30*, 850–859.

Benjamin, A., Zubajlo, R., Thomenius, K., et al. (2017). Diagnosi non invasiva della NAFLD mediante ecogenicità ultrasonografica. *IEEE Engineering in Medicine and Biology Conference*, 2920–2923.

Bril, F., Ortiz-Lopez, C., Lomonaco, R., et al. (2015). Valore clinico dell'ecografia epatica nella diagnosi di NAFLD in pazienti sovrappeso e obesi. *Liver International, 35*(9), 2139–2146.

Brubakk, A. O., & Mollerløkken, A. (2003). Danno endoteliale e infiammazione indotti da bolle: implicazioni per la malattia da decompressione. *Journal of Applied Physiology, 94*(6), 2147–2153.

Brunt, E. M., Kleiner, D. E., Wilson, L. A., et al. (2022). Patologia della NAFLD e della NASH: aggiornamento. *Hepatology, 76*(6), 1880–1893.

Buzzacott, P., & Denoble, P. J. (2018). Mortalità nella subacquea ricreativa: epidemiologia e fattori di rischio. *Undersea & Hyperbaric Medicine, 45*(4), 383–392.

Caussy, C., Reeder, S. B., Sirlin, C. B., & Loomba, R. (2018). Valutazione quantitativa non invasiva del grasso epatico mediante ecografia e risonanza magnetica. *Nature Reviews Gastroenterology & Hepatology, 15*(10), 627–644.

Carotti, S., Morini, S., Corradini, S. G., et al. (2020). Cellule endoteliali sinusoidali epatiche: morfologia, funzione e ruolo nelle malattie del fegato. *Cells, 9*(3), 706.

Cialoni, D., Pieri, M., & Marroni, A. (2017). Predisposizione fisiologica alla malattia da decompressione: ruolo della funzione endoteliale e della microcircolazione. *Frontiers in Physiology, 8*, 1063.

Cialoni, D., Pieri, M., Balestra, C., & Marroni, A. (2017). Fattori di rischio e formazione di bolle nei subacquei ricreativi: analisi del database DSL di DAN Europe. *Frontiers in Psychology, 8*, 1587.

Cialoni, D., Pieri, M., & Marroni, A. (2017). Disfunzione endoteliale e malattia da decompressione: prospettive attuali. *Frontiers in Physiology, 8*, 1063.

Cialoni, D., Pieri, M., & Marroni, A. (2017). Il ruolo del forame ovale pervio e degli shunt polmonari nella malattia da decompressione. *European Journal of Applied Physiology, 117*(11), 2129–2140.

Cialoni, D., Pieri, M., & Marroni, A. (2017). Esposizione iperbarica e stress vascolare subclinico: considerazioni metodologiche. *European Journal of Applied Physiology, 117*(11), 2129–2140.

Cotoi, C., & Quaglia, A. (2016). Aspetti istopatologici della rigenerazione e zonazione epatica. *Hepatology Research, 46*(10), 895–907.

Currens, M. A., Moon, R. E., & Freiberger, J. J. (2025). Attivazione della cascata infiammatoria da bolle intravascolari. *Undersea and Hyperbaric Medicine, 52*(1), 23–34.

Dinani, A., & Sanyal, A. J. (2017). Malattia epatica steatosica non alcolica: epidemiologia, patogenesi e trattamento. *Clinics in Liver Disease, 21*(2), 301–312.

Dioguardi Burgio, M., Ronot, M., Reizine, E., et al. (2023). Ruolo emergente dell'ecografia quantitativa nella valutazione della steatosi epatica. *European Radiology, 33*(8), 5746–5760.

Divers Alert Network (DAN). (2016). *Annual Diving Report 2014–2015*. Durham, NC: DAN Publications.

Doolette, D. J. (2016). Emboli gassosi venosi e malattia da decompressione: legami e limiti. *Undersea & Hyperbaric Medicine, 43*(5), 541–549.

Edmonds, C., Lowry, C., & Pennefather, J. (2016). *Medicina subacquea e subacquea clinica* (5ª ed.). CRC Press.

Eddowes, P. J., Sasso, M., Allison, M., et al. (2019). Accuratezza del parametro CAP e della stiffness epatica nella valutazione della NAFLD. *Gastroenterology, 156*(6), 1717–1730.

Eftedal, O., & Brubakk, A. O. (1997). Rilevazione ecografica di bolle intravascolari: revisione. *Ultrasound in Medicine & Biology, 23*(6), 901–918.

Farrell, G. C., van Rooyen, D., Gan, L., & Chitturi, S. (2012). La NASH come disordine infiammatorio: implicazioni prognostiche e terapeutiche. *Gut and Liver, 6*(2), 149–171.

Géraud, C., Evdokimov, K., Straub, B. K., et al. (2012). Architettura specifica delle giunzioni cellulari nelle cellule endoteliali sinusoidali epatiche. *Journal of Hepatology, 57*(4), 736–749.

Gempp, E., & Blatteau, J. E. (2010). Prevalenza della DCS nella subacquea ricreativa: revisione dei fattori contributivi. *Undersea & Hyperbaric Medicine, 37*(3), 133–140.

Greco, D., Kotronen, A., Westerbacka, J., et al. (2008). Espressione genica nella NAFLD umana. *American Journal of Physiology: Gastrointestinal and Liver Physiology, 294*, G1281–G1287.

Hess, H. W., et al. (2021). Variabilità individuale nella formazione di bolle dopo immersioni standardizzate. *European Journal of Applied Physiology, 121*(10), 2863–2872.

Imbert, J. P., Cialoni, D., Sponsiello, N., et al. (2019). Obesità e disturbi metabolici come modificatori del rischio da decompressione. *Frontiers in Physiology, 10*, 1453.

Imbert, J. P., Egi, S. M., Germonpré, P., & Balestra, C. (2019). Bolle metaboliche statiche come precursori di emboli gassosi vascolari durante la decompressione dei subacquei. *Frontiers in Physiology, 10*, 807.

Jin, R., et al. (2020). Annexin A2 come indicatore di resistenza insulinica e steatosi epatica nella NAFLD. *Metabolism, 107*, 154234.

Karimpour, M., Barak, M., & Arieli, R. (2022). Rilevazione ecografica degli emboli gassosi vascolari post-immersione: attualità e applicazioni cliniche. *Frontiers in Physiology, 13*, 863221.

Khov, N., Sharma, A., & Riley, T. (2014). L'ecografia al letto del paziente nella diagnosi della NAFLD. *World Journal of Gastroenterology, 20*(22), 6821–6825.

Kleiner, D. E., Brunt, E. M., Van Natta, M., et al. (2005). Progettazione e validazione di un sistema istologico per la NAFLD. *Hepatology, 41*(6), 1313–1321.

Lee, D. H., Lee, J. Y., Bae, J. S., et al. (2020). Ecografia quantitativa mediante coefficiente di backscatter per la valutazione della steatosi epatica. *Ultrasound in Medicine & Biology, 46*(7), 1776–1785.

Liang, J., Sun, X., Yi, L., et al. (2022). Effetto della terapia iperbarica sull'iperlipidemia e sul peso corporeo nei ratti. *Biochemical and Biophysical Research Communications, 599*, 106–112.

Liu, W., Baker, R. D., Bhatia, T., Zhu, L., & Baker, S. S. (2010). Patogenesi della steatoepatite non alcolica. *Cellular and Molecular Life Sciences, 67*(19), 3327–3342.

Lonardo, A., et al. (2020). NAFLD e malattie cardiovascolari: revisione comprensiva. *Journal of Internal Medicine, 288*(5), 402–421.

Luangmonkong, T., et al. (2023). Saggi ad alto contenuto per lo studio della funzione mitocondriale nella NAFLD. *Archives of Toxicology, 97*(3), 823–835.

Marchesini, G., & Day, C. P. (2016). Patogenesi della NAFLD: fattori metabolici, genetici e ambientali. *Journal of Hepatology, 64*(2), 696–708.

Mitchell, S. J., & Doolette, D. J. (2013). Fisiopatologia della malattia da decompressione. *Comprehensive Physiology, 3*(3), 1633–1670.

Mitchell, S. J. (2024). Malattia da decompressione: panoramica completa. *Diving and Hyperbaric Medicine, 54*, 1–53.

Nishi, R. Y., & Kisman, K. E. (1988). Valutazione dello stress da decompressione tramite monitoraggio Doppler precordiale. *Undersea Biomedical Research, 15*(1), 27–38.

Papackova, Z., et al. (2015). Resistenza insulinica selettiva in cellule HepG2 steatosiche umane. *BMC Gastroenterology, 15*, 114.

Papadopoulou, V., Eckersley, R. J., Balestra, C., et al. (2018). Dinamica circolatoria delle bolle: dagli aspetti fisici a quelli biologici. *Advances in Colloid and Interface Science, 256*, 239–249.

Parmar, S. R., et al. (2023). Danno epatico mediato dallo stress ossidativo nella steatosi: prospettive terapeutiche. *Frontiers in Pharmacology, 14*, 1122457.

Piscaglia, F., et al. (2022). Intelligenza artificiale in ecografia epatica: evidenze attuali e prospettive future. *Journal of Hepatology, 77*(6), 1682–1695.

Poisson, J., Lemoinne, S., Boulanger, C., et al. (2017). Fisiologia e ruolo delle cellule endoteliali sinusoidali epatiche nelle malattie del fegato. *Journal of Hepatology, 66*(1), 212–227.

Professional Association of Diving Instructors (PADI). (2023). *Annual Certification and Industry Statistics Report.*

Quintana, C. R., Aguirre, M. I., Soto, R. I., et al. (2020). Espressione del gene CD36 nel tessuto adiposo e epatico in modelli animali di steatosi. *Prostaglandins Other Lipid Mediators, 147*, 106404.

Riazi, K., Azhari, H., Charette, J. H., et al. (2022). Prevalenza e incidenza globale della NAFLD: revisione sistematica e meta-analisi. *The Lancet Gastroenterology & Hepatology, 7*, 851–861.

Salam, A., Malik, A., & Farid, N. (2024). Ruolo dell'ecografia nella diagnosi della NAFLD. *Pakistan Journal of Medical and Health Sciences, 17*(12), 1248.

Sanyal, A. J., Campbell-Sargent, C., Mirshahi, F., et al. (2001). Steatoepatite non alcolica: associazione tra resistenza insulinica e anomalie mitocondriali. *Gastroenterology, 120*(5), 1183–1192.

Sasso, M., Beaugrand, M., de Ledinghen, V., et al. (2010). Controlled Attenuation Parameter (CAP): nuovo strumento per la valutazione non invasiva della steatosi. *Journal of Hepatology, 53*(6), 1030–1037.

Spencer, M. P. (1976). Limiti di decompressione e relazione con emboli gassosi venosi rilevati mediante Doppler. *Undersea Biomedical Research, 3*(3), 253–260.

Takahashi, Y., & Fukusato, T. (2014). Istopatologia della steatosi epatica non alcolica. *World Journal of Gastroenterology, 20*(42), 15539–15548.

Tandra, S., Yeh, M. M., & Brunt, E. M. (2011). Patologia della NAFLD: panoramica generale. *Clinics in Liver Disease, 15*(1), 11–26.

Targher, G., & Byrne, C. D. (2021). NAFLD e rischio cardiovascolare: meta-analisi. *The Lancet Gastroenterology & Hepatology, 6*(11), 903–917.

Valić, Z., et al. (2005). Uso dell'ecocardiografia e del Doppler per la rilevazione non invasiva di emboli gassosi nei subacquei. *Clinical Physiology and Functional Imaging, 25*(6), 348–352.

Vann, R. D., Butler, F. K., Mitchell, S. J., & Moon, R. E. (2011). Malattia da decompressione. *The Lancet, 377*(9760), 153–164.

Venidiktova, D., Borsukov, A., Alipenkova, A. V., et al. (2019). Steatometria ecografica in pazienti con NAFLD: risultati preliminari. *Journal of Clinical Practice, 10*(1), 23–29.

Webb, M., Yeshua, H., & Zelber-Sagi, S. (2009). Valore diagnostico dell'indice epatorenale computerizzato nella valutazione della steatosi. *Journal of Hepatology, 51*(6), 1069–1076.

Xu, R., Tao, A., Zhang, S., & Chen, G. (2024). NAFLD e disfunzione endoteliale: meccanismi che collegano fegato e malattia vascolare. *Frontiers in Cardiovascular Medicine, 11*, 1378945.

Younossi, Z. M., et al. (2019). Epidemiologia globale della NAFLD. *Nature Reviews Gastroenterology & Hepatology, 16*(1), 11–20.

Zehlicke, T., et al. (2016). Confronto tra algoritmi decompressivi mediante monitoraggio post-immersione delle bolle. *Diving and Hyperbaric Medicine, 46*(2), 69–75.